博士（医学）論文
Doctor's Thesis

The roles of B-Raf
in TCR-mediated T cell activation in human T cells

TCR を介した T 細胞活性化シグナル伝達における B-Raf の機能解析

粟井（塚本）博丈
Hirotake Tsukamoto Awai

熊本大学大学院医学研究科
脳・免疫統合科学系専攻免疫識別学
（指導：西村　泰治　教授）

2006 年 3 月

Doctor's Thesis

The roles of B-Raf
in TCR-mediated T cell activation in human T cells

Hirotake Tsukamoto Awai

Supervisor

Yasuharu Nishimura

Department of immunogenetics,
Graduate School of Medical Sciences,
Kumamoto University

March 2006

1. Contents

2. Summary

The interactions between low-avidity peptide/MHC complexes and its cognate TCRs are essential for the positive selection of thymocytes, and the survival and homeostatic proliferation of peripheral T cells. However, the detailed relationship between the avidity of TCR ligand and the subsequent intracellular signaling through the TCR is still unclear. To investigate the effects of TCR ligand avidity on TCR-mediated signaling, we established the L cells expressing human histocompatibility leukocyte antigen (HLA)-DR4 molecules covalently linked with agonistic peptide (high-affinity ligand) or altered peptide ligand (APL; low-affinity ligand) at various densities as antigen presenting cells (APC) for a cognate human T cell clone. Using this system, we demonstrated that the up-regulation of CD69, interleukin-2 production and proliferation but not detectable phosphorylation of ZAP-70/LAT/SLP-76 were provoked in human $CD4^+$ T cell clone stimulated with low-avidity interactions by APL/HLA-DR4 complexes presented at an excessive density. In contrast to the high-avidity stimulation, the stimulus evoked delayed and sustained activation of the B-Raf/Extracellular signal-regulated kinase (ERK) pathway without Raf-1 activation. The strength and duration of B-Raf/ERK activations correlated closely with the density of the TCR ligand. Loss-of-function analyses confirmed that B-Raf plays an indispensable role in both agonist-induced and APL-induced T cell activations, and in the latter situation, B-Raf dependency was more striking. These observations suggest that the differences in avidity of TCR-peptide/MHC interactions modulate the strength and duration of the B-Raf/Raf-1/ERK activation in the human $CD4^+$ T cells.

Furthermore, we investigated the roles of B-Raf in TCR-mediated IL-2 production coupled with ERK activation in Jurkat human T cell line. We found that TCR cross-linking could induce up-regulation of both B-Raf and Raf-1 activities, but Raf-1 activity was decreased rapidly. On the other hand, TCR-stimulated kinase activity of B-Raf was sustained. Expression of a dominant-negative mutant of B-Raf abrogated sustained but not transient TCR-mediated MEK/ERK activation. The inhibition of sustained ERK activation by either expression of a dominant-negative B-Raf or treatment with a MEK inhibitor resulted in a decrease of the TCR-stimulated nuclear

factor of activated T cells (NFAT) activity and IL-2 production. Collectively, our data provide the first time direct evidence that B-Raf is a positive regulator of TCR-mediated sustained ERK activation, which is required for NFAT activation and the full production of IL-2.

3. Publication list

1) H. Tsukamoto, A. Irie, YZ. Chen, JR Kim, K. Takeshita and Y. Nishimura
TCR ligand avidity detemines the mode of B-Raf/ERK activation leading to proliferative response in a human $CD4^+$ T cell clone (revised in *Eur. J. Immunol*.)

2) H. Tsukamoto, A. Irie and Y. Nishimura.
B-Raf contributes to sustained extracellular signal-regulated kinase on associated with interleukine-2 production stimulated through T cell receptor. ***J. Biol. Chem.*** 279: 48457-48465, 2004

3) J-R. Kim, A. Irie, H. Tsukamoto, Y. Nishimura
An important role of unphosphorylated ZAP-70 associated with partially phosphorylated TCR-z chain for T cell activation induced with altered peptide ligand simulation. ***Biochem. Biophys. Res. Comm.,*** in Press

4) Y. Yoshitake, T. Nakatsura, M. Monji, S. Senju, H. Matsuyoshi, H. Tsukamoto, S. Hosaka, H. Komori, D. Fukuma, Y. Ikuta, T. Katagiri, Y. Furukawa, H. Ito, M. Shinohara, Y. Nakamura and Y. Nishimura.
Proliferation potential-related protein, an ideal esophageal cancer antigen for immnotherapy identified using cDNA microarray analysis. ***Clinical Cancer Research*** 10: 6437-6448, 2004

5) Y. Nishimura, Y-Z. Chen, Y. Uemura, Y. Tanaka, H. Tsukamoto, T. kanai, H. Yokomizo, C.Yun, T. Matsuoka, A. Irie and S. Matsushita.
Degenerate recognition and response of human $CD4^+$ Th cell clones: implications for basic and applied immunology ***Mol. Immunol.*** 40: 1089-1094, 2004

6) Y. Uemura, S. Senju, K. Maenaka, L. K. Iwai, S. Fujii, H. Tabata, H. Tsukamoto, S. Hirata, Y. Z. Chen, and Y. Nishimura.

Systematic analysis of the combinatorial nature of epitopes recognized by TCR leads to identification of mimicry epitopes for glutamic acid decarboxylase 65-specific TCRs. ***J. Immunol.*** 170: 947-960, 2003

7) A. Irie, Y-Z Chen, H. Tsukamoto, T. Jotsuka, M. Masuda and Y. Nishimura
Unique T cell proliferation associated with PKC activation and impaired ZAP-70 phosphorylation in recognition of overexpressed HLA/partially agonistic peptide complexes. ***Eur. J. Immunol.*** 33: 1497-1507, 2003

8) T. Yamane, T. Kunisada, H. Tsukamoto, H. Yamazaki, H. Niwa, S. Takada and S. Hayashi
Wnt signaling regulates hemopoiesis through stromal cells. ***J. Immunol.*** 167:765-772, 2001

9) 塚本博丈, 西村泰治
「CLIP 置換型インバリアント鎖遺伝子を利用したペプチド/MHC-II 複合体発現細胞システムの構築」, ***Medical Science Digest***, ニュ－サイエンス社, 31(5): 5-6, 2005.

10) 塚本博丈, 西村泰治
「MHC による抗原提示」, バイオ研究マスターシリーズ 免疫学集中マスター, 羊土社, 84-92, 2005.

4. Acknowledgments

These series of investigations were performed from 2001 to 2006, in the Department of Immunogenetics, Graduate School of Medical Sciences, Kumamoto University.

I wish to extend my warmest thanks to Professor Yasuharu Nishimura, professor of the department of the Department of Immunogenetics, Graduate School of Medical Sciences, Kumamoto University. He generously gave me advice and suggestions. I would also like to express my gratitude for his spending valuable time to correct my papers.

I am also grateful to Dr. Atsushi Irie, Dr. Satoru Senju, and all members in the Department of Immunogenetics, Graduate School of Medical Sciences, Kumamoto University, who provided me valuable advices. I also would like to thank Ms. Midori Fukuda for her secretarial assistance.

I thank Dr. K. L. Guan for the generous gift of B-Raf constructs, Dr. V. A. Boussiotis for IL-2 promoter-luciferase reporter construct, Dr. R. M. Niles for AP-1-luciferase reporter construct, Dr. T. Saito for NFAT-GFP reporter construct, Dr. Y. Takai for GST-MEK expression construct, and Dr. G. R. Crabtree for TAg-Jurkat cells, Dr. T. Kinashi for RalGDS-GST construct, Dr. Ronald C. Desrosiers for *Herpesvirus saimiri* and OMK cell lines, Dr. T. Ejima for rhIL-2 and Dr. H. Miyoshi for lentiviral vector system. We also acknowledge Dr. Masaki Yasukawa for helpful discusssion about HVS transformation methods. These works was supported in part by Grants-in-Aid Nos. 12051203, 14370115 and 15510165 from the Ministry of Education, Science, Technology, Sports, and Culture, Japan.

Finally, I acknowledge my wife, Maiko and greatly appreciate her warm encouragement.

5. Abbreviations

APC, antigen presenting cell;
APL, altered peptide ligand;
AP-1, activating protein-1;
cDNA, complementary DNA;
DMSO, dimethylsulfoxyde;
EGFP, enhanced green fluorescent protein;
ELISA, enzyme-linked immunosorbent assay;
ERK, extracellular signal-regulated kinase;
FITC, fluorescein isothiocyanate;
GST, glutathione S-transferase;
HA, hemaggulutinin;
HLA, human histocompatibility leukocyte antigen;
HRP, horseradish peroxidase;
HVS, *Herpesvirus saimiri*;
IL-2, interleukin-2;
LAT, linker for activation of T cells;
mAb, monoclonal antibody;
MAPK, mitogen-activated protein kinase;
MEK, MAPK/ERK kinase;
MHC, major histocompatibility complex;
mRNA, messenger RNA;
NFAT, nuclear factor of activated T cells;
PBMCs, peripheral blood mononuclear cells;
PCR, polymerase chain reaction;
PE, phycoerythrin;
PMA, phorbol 12-myristate 13-acetate;
RT-PCR, reverse transcriptase-PCR;
SDS-PAGE, sodium dodecylsulfate polyacrylamide gel electrophoresis;
SLP-76, SH2 domain containing leukocyte-specific phosphoprotein of 76 kDa;
TCR, T cell receptor;
ZAP-70, □ chain-associated protein 70 ;

6. Introduction

6.1 Biological significance of T cell responses stimulated with low avidity TCR ligand

A T cell receptor (TCR) recognizes not only foreign antigenic peptides with high-affinity but also the endogenous self peptides with low-affinity in the context of the self major histocompatibility complex (MHC) molecule (1,2). The avidity between the TCR and peptide/ MHC is the sum of the affinity of the TCR to peptide/MHC complex, and such avidity depends on the abundance of the TCR ligands expressed on antigen presenting cells (APCs) (Fig.1). Numerous studies support the view that the functional outcomes of T cells and the subsequent generation of the adaptive immune responses depend on the avidity of these TCR-peptide/MHC interactions (1-3).

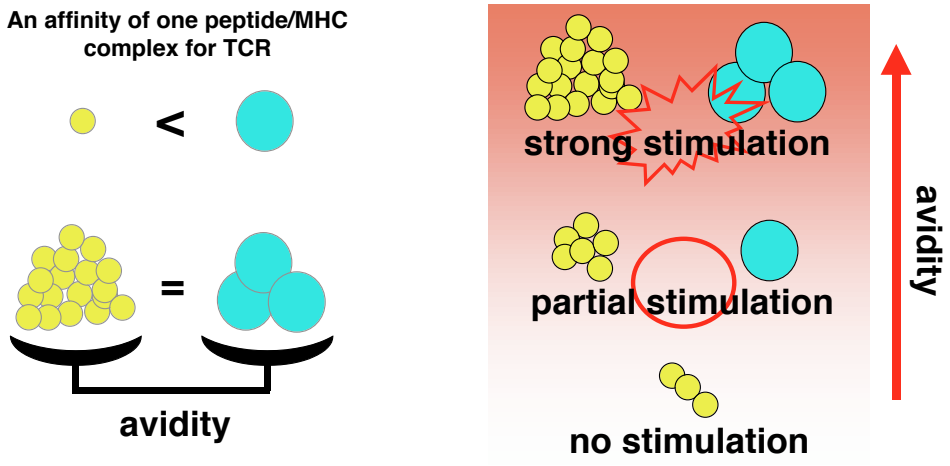

Fig. 1 TCR-mediated responses are dictated with ligand avidity

The left figure compares the ligand affinity for TCR. The size of circle indicates a binding affinity of one peptide/MHC complex for TCR. The avidity between the TCR and peptide/ MHC is the sum of the affinity of the TCR to peptide/MHC complex. TCR signals triggered with numerous low affinity ligands accumulate, resulting in achieving identical magnitude of TCR signals that evoked by the stimulation with high affinity ligand. Thereby, the T cell responses depend on the avidity of TCR ligation.

The stimulus of low-affinity/avidity interaction with TCR play crucial roles in the induction of incomplete signals leading to diverse T cell responses. As shown in Fig. 2, in the thymus, thymocytes with high-avidity self-specific TCRs receives the strong signal and are eliminated (negative selection), whereas a fraction of the cells

recognizing self-peptide/MHC complexes with low-avidity receives the weak signal and differentiates into a mature CD4/8 single positive stage (positive selection) (2). In the periphery, T cell recognition by TCR of self peptide/MHC complexes with low-avidity helps to maintain the peripheral T cell homeostasis such as self tolerance (1), survival (4,5), homeostatic proliferation of naive and memory $CD4^+$ T cells (6), and the augmentation of the sensitivity toward foreign antigenic peptides (7). These functional characteristics are quite similar to the T cell responses induced by some altered peptide ligands (APLs) with low-affinity/avidity for cognate TCR that have amino acid substitution(s) in agonistic peptides. Such subtle changes in the structure of TCR ligands fail to induce the full T cell activation (3,5,8), but give rise to the partially agonistic property that effectively elicits the positive selection of thymocytes (9), regulates the cytokine production profile (10,11) and promotes the survival (5) and homeostatic proliferation of peripheral T cells (12).

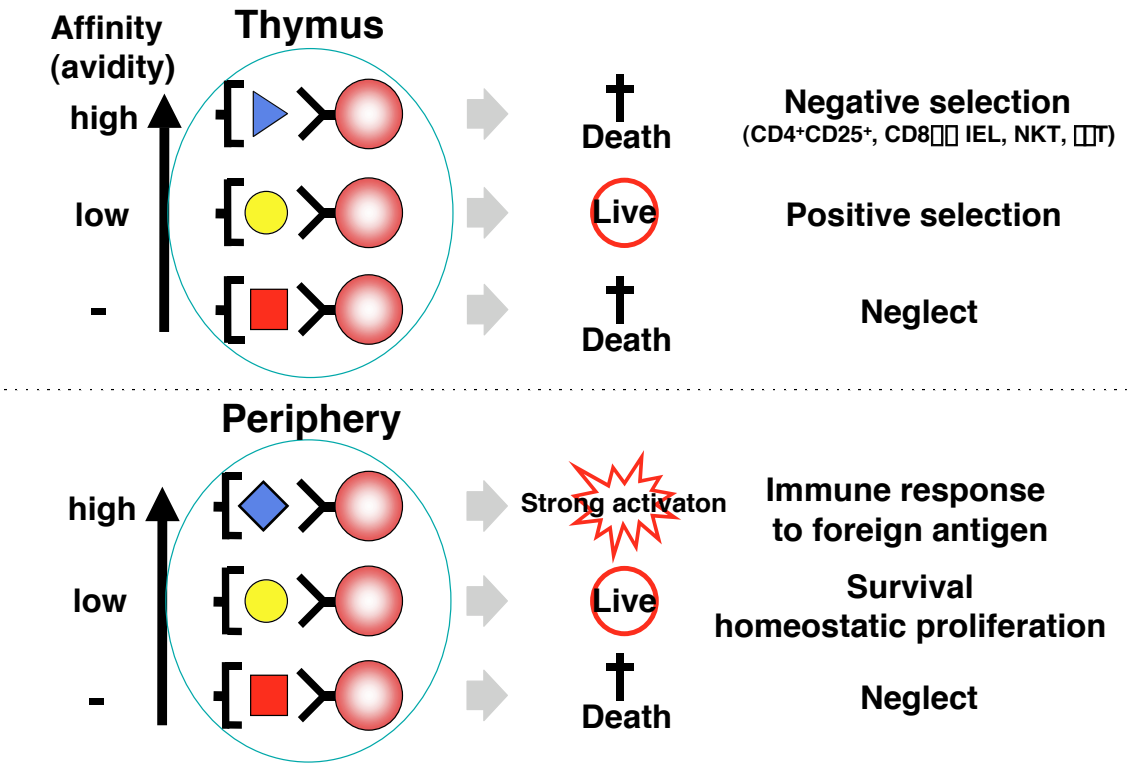

Fig. 2 Difference of TCR ligand avidity regulate the diverse responses of T cells.

The ligand affinity/avidity for TCR is one of the important factors in determining the fate of T cells in

thymus and periphery in vivo. See text for details.

6.2 TCR-mediated signal transduction

Regarding the intracellular signaling events through the TCR, our understanding of the TCR-mediated signaling pathways initiated by encountering antigenic peptide/MHC complex presented by APCs has largely been based on the results of studies in which TCR engagement is mimicked using reagents such as anti-CD3 antibodies. The stimulation by crosslinking the CD3 molecules with anti-CD3 monoclonal antibody (mAb) or the TCR engagement of agonistic peptide/MHC complex provide a high-avidity signal, inducing tyrosine phosphorylation of CD3-ζ chain, ζ chain-associated protein 70 (ZAP-70) and downstream signaling molecules (3). On the other hand, the stimulation with low-affinity APL/MHC complexes provide a low-avidity signal, resulting in incompletely phosphorylated CD3-ζ chains, impaired phosphorylation of ZAP-70 (1,3,13-15) and altered intracellular calcium responses (14,16) (Fig. 3). Although low-affinity APLs appear to induce incomplete or differential signaling events in T cells (13-15), because of its subtle intracellular signals under physiological situations, the relationship between the nature of TCR ligation and resulting signal transductions though the TCR remains unclear.

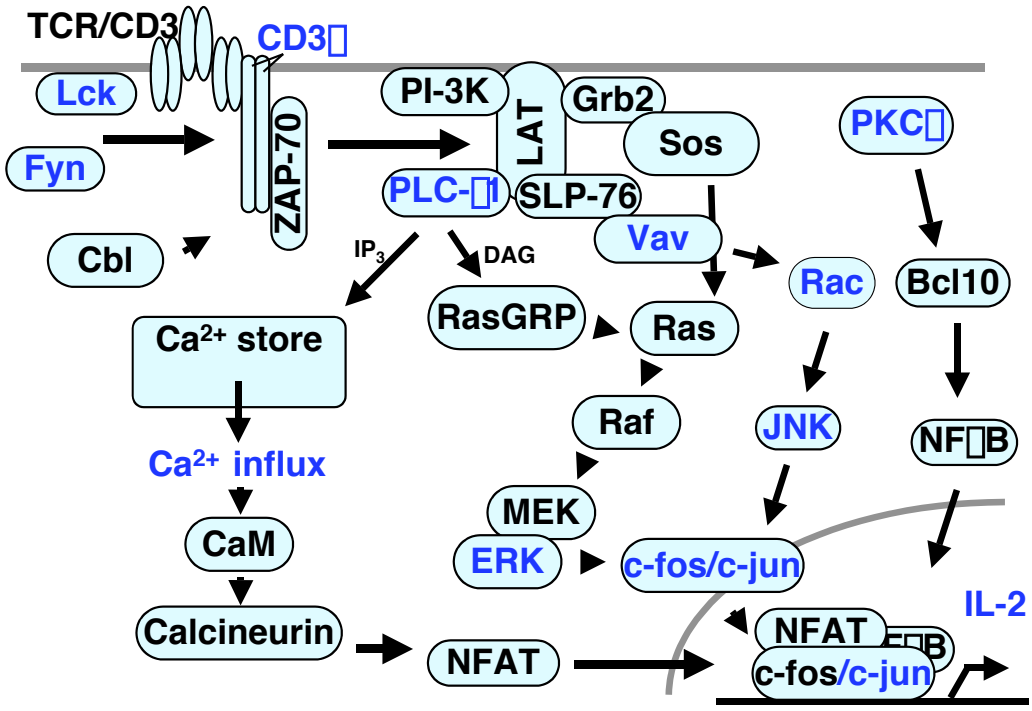

Fig. 3 Schematic model of TCR signaling

The molecules indicated by gray letters indicate the signaling molecules that were previously reported to be regulated with low avidity TCR ligand.

6.3 Hypotheses and experimental systems

When T cells were activated by recognizing a few cognate peptide/MHC complexes on APC, it has been suggested that a single peptide/MHC complex can serially engage multiple number of TCR (17). However, it is hypothesized that the sub-threshold density of an incompletely stimulatory peptide/MHC that have short half-life of interaction with TCR is incapable of transducing the productive signals and inducing full T cell activation (17,18) (Fig. 4). Thus, to investigate the effect of TCR ligand avidity on TCR-mediated signaling, we have established a series of L cell transfectants expressing various number of single agonistic peptide or low-affinity APLs covalently linked with human histocompatibility leukocyte antigen (HLA) class II molecule (15,19), since loading with an exogenously added peptide on cognate MHC molecules cannot be completely attained (20,21) (Table 1 and Fig. 5). Utilizing this system, we previously found that an excessive presentation of the some APL/HLA-DR4

complexes induced interleukin (IL)-2 production and proliferation with a similar degree to the case of stimulation with high-avidity TCR interactions in the cognate human $CD4^+$ T cell clone. However, in contrast to the high-avidity stimulation, this responses induced by the APL/HLA-DR4 complexes was not accompanied with the activation of ZAP-70 nor detectable tyrosine phosphorylation of linker for activation of T cells (LAT), suggesting the differential stimulatory capacity of the excessively presented low-affinity TCR ligand and the presence of alternative signaling pathway(s) to elicit the T cell activation (15).

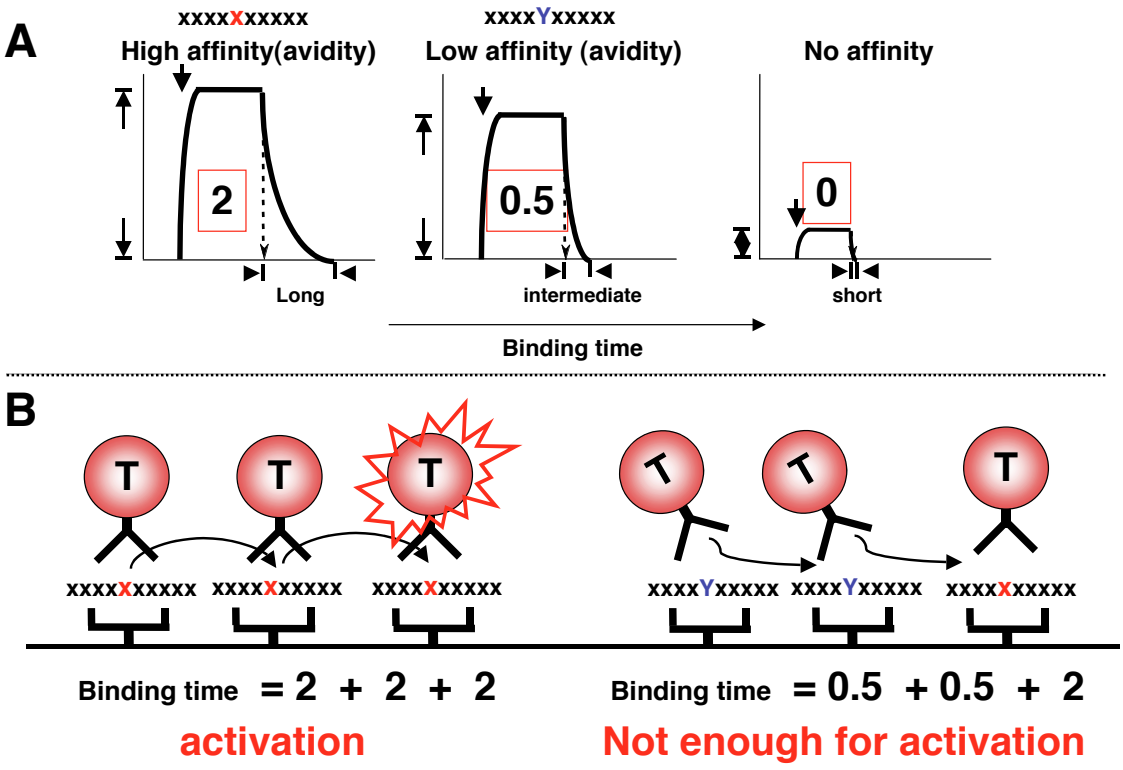

Fig. 4 Serial triggering model in T cells recognizing the differential affinity TCR ligand.

A, The kinetics of interaction between TCR and TCR ligand, a molecular complex of peptide and MHC. High affinity ligand associates with TCR for long time. On the other hand, the interaction of low affinity ligand with TCR exhibits a shorter life span. B, Schematic depiction of serial interaction between a TCR and high or low affinity ligand on the surface of an APC. Long interaction of TCR with some high affinity ligands can induce substantial T cell activation, whereas short interaction with some low affinity ligands is not enough to provoke the T cell activation.

Table 1. TCR ligands for T5-32; M12p54-68 and its analogue peptide Q59G

peptide	sequence	antigenicity
M12p54-68	NRDLEQAYNELSGEA	full agonist
Q59G	NRDLEGAYNELSGEA	antagonist

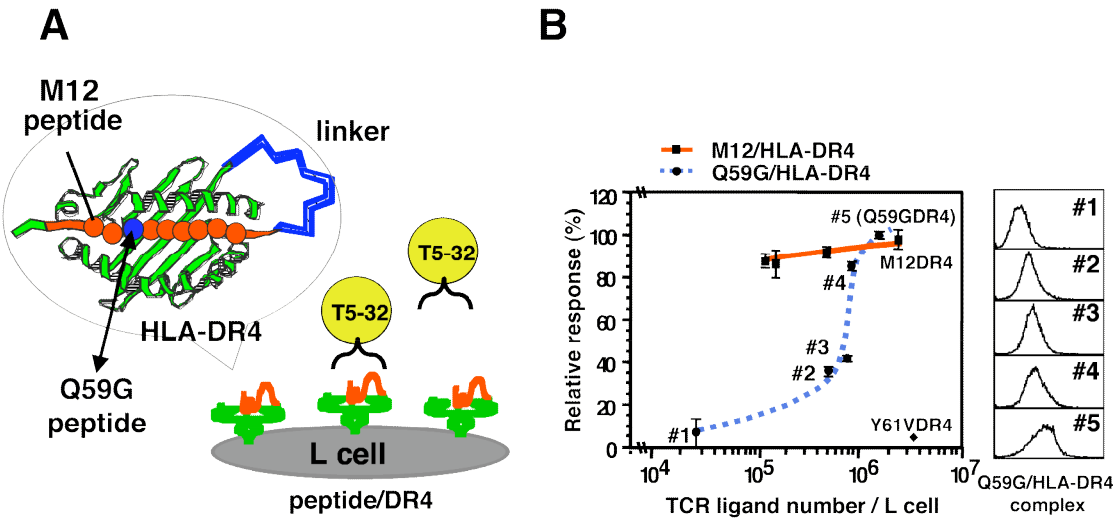

Fig. 5 The experimental materials used in this study

A, L cells expressing agnistic peptide, M12 or its single amino acid substituted variant Q59G covalently linked with HLA-DR4 molecule were used as APCs for cognate T cell clone, T5-32 in this study. B, T5-32 was stimulated with L cell transfectants which expressed M12 or its APLs covalently linked with HLA-DR4 molecule at high density. The proliferation of T5-32 stimulated with the indicated L cells was determined by [^{3}H] thymidine incorporation. Each relative response was normalized when the response of T5-32 stimulated with M12DR4 was assigned to be 100% (left panel). The L cell clones expressing each peptide/HLA-DR4 complex that induced a maximal response of T5-32 are defined as M12DR4 and Q59GDR4, respectively. The density of Q59G/HLA-DR4 complex was estimated by anti-HLA-DR antibody in each L cell clones (designated as #1-5 in the right panel). The dotted line showed in the FACS profile of #1 indicated the profile of cells stained with isotype-matched antibody as a negative control. The details are described in Result section in below.

In this study, we extend the previous study and herein characterized the alternative signaling pathway(s) that contribute to the activation induced by TCR engagement with the relatively low-avidity TCR ligand. This stimulus provoked the altered kinetics of B-Raf/Raf-1/Extracellular signal-regulated kinase (ERK) activation different from that stimulated with the agonistic high-avidity interactions. Furthermore, the strength and duration of B-Raf/ERK activities depended on the density of the altered TCR ligand and were correlated with the magnitude of T cell proliferation. Our data indicate that differences in TCR ligand avidity altered the mode of B-Raf/Raf-1/ERK activation, which plays crucial roles in the T cell activation.

6.4 TCR-mediated ERK activation and Raf family kinases

Regarding TCR-mediated signal transduction, one well-studied key switch is the activation signal of extracellular signal-regulated kinase (ERK) 1/2, which is mediated by small GTP-binding protein, Ras (22,23) and Rap1 (24,25) (Fig. 3). Current models suggest that TCR stimulation with the agonistic peptide/MHC complex activates the conversion of Ras from GDP- to GTP-bound form (22,26). Activated Ras subsequently recruits the serine/threonine kinase Raf-1 to the plasma membrane, resulting in its activation. Activated Raf-1 then activates ERK kinase (MEK), which directly phosphorylates tyrosine and threonine residues (TEY motif) on ERK1/2 to activate them (26). These signals combine to activate multiple transcription factors, including nuclear factor of activated T cells (NFAT), nuclear factor-kappa B (NF-*k*B) and activating protein-1 (AP-1), all of which contribute toward the production of IL-2 (Fig. 3 and Raf. (27-29)).

ERK1/2 are involved in a diverse array of cellular functions including cell growth and apoptosis of T cells (30-32). In ERK1-deficient mice, the thymocyte differentiation from $CD4^+CD8^+$ double positive to the $CD4^+/CD8^+$ single positive stage is impaired, thus ERK activation by TCR ligation plays important roles in T cell development (33). Experiments using pharmacological inhibitors of MEK and dominant negative MEK also provided evidence that ERK1/2 are critical for thymocyte differentiation (31,34) and for induction of TCR-mediated mitogenic signals and IL-2 production in mature T cells (27,35). Hence, it is important to understand how the

strength and duration of ERK activity is regulated in TCR-mediated activation and fate decisions of T cells.

6.5 Objectives of this work

The functions of ERK signaling are regulated by its upstream elements, in particular by members of the Raf-family in various cell types and three Raf isoforms, Raf-1, A-Raf and B-Raf, are expressed in mammalian cells (Fig. 6 and Ref. 36 and 37). Whereas Raf-1 is ubiquitously expressed, B-Raf shows a more restricted expression pattern (38), 39). Mice deficient in the different Raf isoforms exhibit different developmental defects, suggesting the non-redundant function(s) of each Raf isoform (40). A different phenotype of each Raf deficient mouse is expected to be due, at least in part, to their distinct expression pattern. It was reported that B-Raf exhibits a much more basal kinase activity and a higher affinity towards MEK than does Raf-1 in vitro (41). Despite these differences, the specific function(s) in vivo, if any, of each Raf isoform is poorly understood. B-Raf was reported to be one component of the receptor-mediated MEK/ERK activation pathway in fibroblasts, B cell lines and PC12 cells (41-46). Moreover, B-Raf expression in T cells is controversial; in this study, we detected B-Raf protein in Jurkat cells and primary human T cells, while others failed to do so (24).

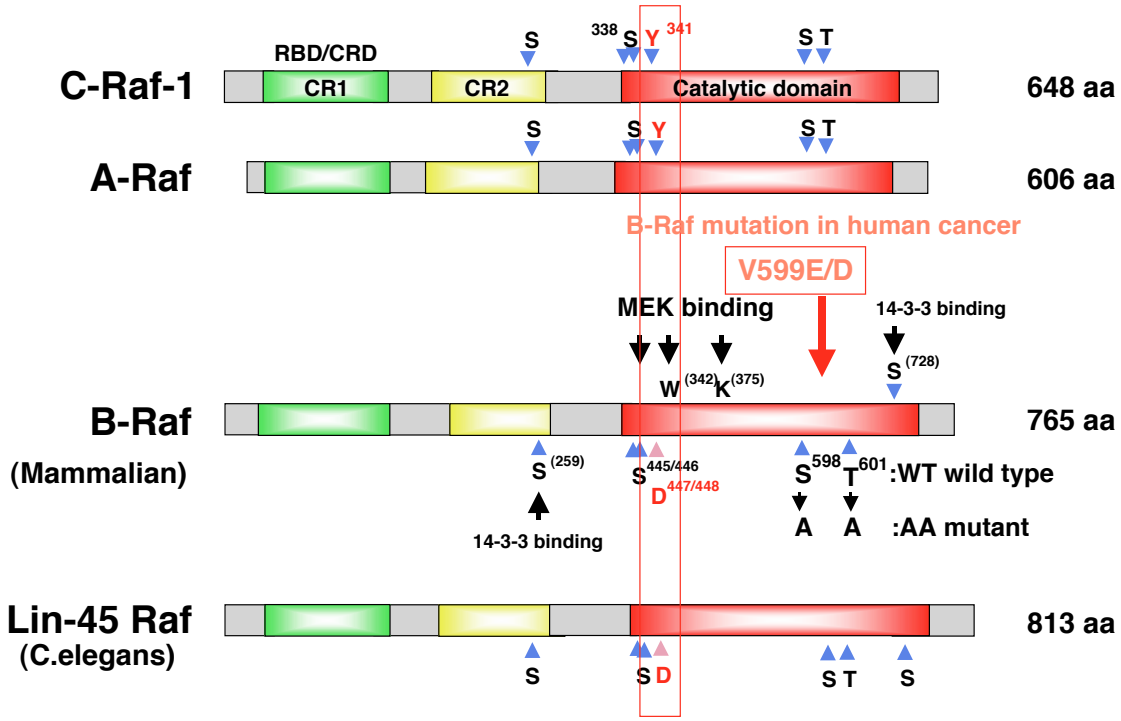

Fig. 6 The structure of Raf family proteins including mammalian Raf, C-Raf, A-Raf and B-Raf, and Lin-45 Raf (C. elegans Raf).

The serine, threonine and tyrosin phosphorylation sites are indicated in the structure. Threonine 598 and Serine 601 in B-Raf are pivotal phosphorylation sites that regulate the kinase activity, and substitution of these sites to Alanine result in dominant negative mutant of B-Raf. The position 599 is also important for kinase activity, and this site is mutated from Valine to acidic amino acid, resulting in its constitutive activity and this mutation is frequently observed in melanoma cells. CR; cystein rich domain

Although Raf-1 is a well-characterized effecter molecule for ERK activation in the TCR-mediated signaling cascade and IL-2 production in T cells (47), much less attention has been directed to the roles of B-Raf in T cells. We report that interaction of B-Raf with MEK and B-Raf activity are induced in a TCR stimulation-dependent manner in Jurkat cells. Our data suggest that MEK/ERK activity are selectively regulated through the Ras/B-Raf signaling pathway and that the sustained B-Raf/MEK/ERK activation is indispensable for the translocation of NFAT into nucleus and for the production of IL-2.

7. Materials and Methods

7.1 Preparation of cells and reagents

Primary human $CD4^+$ T cells from healthy donor and primary mouse $CD4^+$ T cells from spleen of C57BL/6 mice were positively isolated with anti-human CD4 and anti-mouse CD4 magnetic beads (Miltenyi Biotec, Aubur, CA), respectively. Human $CD4^+$ T cell clone, YN5-32 was generated in our laboratory as described (8). YN5-32 and T5-32 (see below) recognize the peptide M12p54-68 (NRDLEQAYNELSGEA) derived from the streptococcal M protein in the context of HLA-DR4 (DRA/DRB1*0406). The APLs in this study have single amino acid substitution at the indicated position of M12p54-68 (8). L cells stably expressing HLA-DR4 molecule or expressing peptides covalently linked with the HLA-DR4 molecule complex were established previously (15). The surface number of each peptide/HLA-DR4 complex on the L cell was quantified using Quantum Simply Cellular™ microbeads (Flow Cytometry Standards).

The owl monkey kidney (OMK) cell line and *Herpesvirus saimiri* (HVS) C488 strain were provided from Ronald C. Desrosiers. The recombinant human (rh) IL-2 was from T. Ejima of Ajinomoto Inc. Jurkat cell clone, E6-1 from the American Type Culture Collection and Jurkat cells expressing simian virus 40 large T antigen (TAg-Jurkat) (48) were maintained in RPMI-1640 medium supplemented with 10% FCS, 2mM L-glutamine, and penicillin-streptomycin (100 U/ml and 100 mg/ml, respectively). Jurkat cells stably expressing a wild-type or a dominant negative form of B-Raf were established and maintained in RPMI /10% FCS with 2 mg/ml G418. The human $CD4^+$ T cell clone, YN 5-32 and peripheral blood mononuclear cells (PBMC) were prepared as described (8,15). For transient and stable transfection, $2x10^7$ Jurkat cells were resuspended in 500 μl of cytomix (49) with the appropriate cDNAs (40 μg). The amount of plasmid DNA was held at 40 μg constant by addition of the pcDNA3 vector control. Cells were electroporated in 280 V at a capacitance of 960 μF. Transfectants were analyzed for CD3 and CD28 expression using flow-cytometry (Becton-Dickinson, Mountain View, CA).

Fluorescein isothiocyanate (FITC) or phycoerythrin (PE)-conjugated anti-CD4,

CD25, CD69 antibodies, anti-CD3 mAb (UCHT-1), anti-CD28 (clone L923) antibody and rabbit polyclonal anti-GFP antibody were purchased from PharMingen (San Diego, CA) and anti-TCR Vβ-20 antibody was from Beckman Coulter. Anti-mouse IgG (Fab specific) antibody was from Sigma (St Louis, MO). Anti- NFAT1, NFAT2, K-Ras, Rap1, B-Raf, Vav1 c-Fos, Lamin B and ERK1 antibodies were obtained from Santa Cruz Biotechnology (Santa Cruz, CA). Anti-MAPK/ERK kinase (MEK), phospho-ERK, Raf-1, MEK, p38 antibodies and a MEK inhibitor U0126 were purchased from Cell Signaling Technology (Beverly, MA). Mouse monoclonal anti-hemaggulutinin (HA) antibody was from Covance (Berkeley, CA). Anti-phospho-tyrosine antibody 4G10 and anti-SH2 domain containing leukocyte-specific phosphoprotein of 76 kDa (SLP-76) antibodies were obtained from Upstate Biotechnology (Lake Placid, NY). Monoclonal anti-Raf-1 antibody was from Transduction Laboratories. Anti-mouse IgG (Fab specific), phorbol 12-myristate 13-acetate (PMA) and mitomycin C were from Sigma (St Louis, MO). Cy3-labeled anti-rabbit Ig antibody, HRP-conjugated rabbit anti-mouse and donkey anti-rabbit IgG were from Amersham Bioscience (Arlington Heights, IL) and rabbit anti-sheep IgG was from Southern Biotechnology Associates (Birmingham, AL). Anti-human IL-2 antibodies were from R&D Systems (Minneapolis, MN). Recombinant glutathione S-transferase (GST)-MEK was prepared as reported (50).

The pcDNA3 expression vectors with HA-tagged wild-type and dominant negative mutant B-Raf cDNAs were provided by Dr. K. L. Guan (51). The RasN17 expression vector and the vector for RalGDS-GST fusion protein were a gift from Dr. T. Kinashi (25). The luciferase reporter construct for IL-2 promoter and AP-1 binding site were kindly provided by Dr. V. A. Boussiotis (52) and Dr. R. M. Niles. (53), respectively. The expression vector for GST-MEK was a gift from Dr. Y. Takai (50). NFAT- green fluorescence protein (GFP) reporter construct, consisting of three tandem NFAT-binding sites followed by a gene encoding GFP, was provided by Dr. T. Saito (54).

7.2 Cell culture and transformation of human $CD4^+$ T cell clone with HVS

YN5-32 was grown in RPMI (Invitrogen, Carlsbad, CA) supplemented with 100 U/ml rhIL-2 and 10% heat inactivated human plasma. The L cell transfectants and OMK cells were maintained in DMEM (Invitrogen) supplemented with 10% FCS. The culture supernatant of OMK cells lytically infected with HVS was filtrated and used as a source of the HVS virus solution. YN5-32 stimulated for 2 days by irradiated autologous peripheral blood mononuclear cells (PBMCs) pulsed with M12p54-68 were infected with HVS. The cells were maintained in the culture medium with 100 U/ml of rhIL-2 for 3 weeks. The outgrowing cells were established and designated as T5-32. The transformation of T5-32 was confirmed by detecting a virus-specific *Tip* gene (55). T5-32 was maintained in RPMI medium supplemented with 20% FCS, 100 U/ml rhIL-2 at 37 ℃ and 5% CO_2 without periodical stimulation with irradiated and peptide-pulsed PBMCs. T5-32 cells exhibited the same expression levels of clonotypic TCR (V□-20), CD3, CD4 and CD28 as those of parental YN5-32 except for a higher expression of CD25. The cells were kept cultured at a density of 0.1-0.5 x 10^6 cells/ml.

7.3 Stimulation of cells

In experiments for stimulation with soluble anti-CD3 antibody for cross-linking, Jurkat cells were incubated on ice for 20 min, and then incubated with anti-CD3 antibody (0.25 □g/ml) for 10 min followed by addition of anti-mouse IgG antibody (1 □g/ml) for 5 min. After the indicated time of incubation at 37 ℃, cells were harvested, and lysed with lysis buffer (see below). For the analysis of promoter activity and IL-2 production, Jurkat cells (1 x 10^6/well) were stimulated with immobilized anti-CD3 and CD28 antibodies (5 □g/ml and 10 □g/ml, respectively). For experiments with inhibitor treatment, cells were preincubated for 30 min with the MEK inhibitor U0126 or dimethylsulfoxyde (DMSO) as a control. In the time course analyses of the effect of ERK activation on IL-2 production by the treatment with U0126, medium containing U0126 or DMSO was added at the indicated time points.

7.4 Evaluation of T cell activation

T5-32 left in FCS- and IL-2-free RPMI for 12 h were used in all assays. The proliferative response of T cells was quantified as described previously (15). Briefly, L cell transfectants expressing HLA-DR4 covalently-linked with peptides were treated with 20 mg/ml mitomycin C at 37 ℃ for 1 h and plated in 96-well plates ($8.0x10^4$/well). After 48 h of co-culture with T5-32 ($4.0 x10^4$), 1 μCi of [^{3}H] thymidine was added and the incorporated radioactivity was counted using a Micro beta counter (Wallac) 24 h later. IL-2 production was quantified by ELISA as described (56). The expression of cell surface markers on T cells was estimated by flow cytometric analyses using FACScan (BD Biosciences). For single cell analyses of ERK phosphorylation, cells were stained for CD4 and then fixed in 1% formaldehyde for 10 min on ice. They were washed, and then permeabilized with 90% methanol for 30 min on ice. Phospho-ERK was detected with anti-phospho-ERK antibody, followed by Cy3-labeled anti-rabbit Ig. IL-2 production by T cells stimulated with the indicated L cells and 1 μg/ml soluble anti-CD28 antibody (BD Pharmingen) for 6 h was also monitored by an IL-2 secretion assay according to the instruction of Miltenyi Biotec with minor modification (Aubur, CA).

7.5 Western blotting, immunoprecipitation and In vitro kinase assay

In the analyses using T5-32, starved T5-32 in FCS- and IL-2-free medium overnight were used. After the indicated time of co-culture with the indicated L cells, the T cells were recovered and lysed in lysis buffer (1% Triton X-100, 150 mM NaCl, 20 mM Tris, pH 7.4, 2 mM EDTA, 10% glycerol, 0.25% sodium deoxycholate, 1 mM sodium orthovanadate, 25 mM β-glycerophosphate, 2 mM sodium pyrophosphate, a protease inhibitor tablet and 10 mM NaF) for 30 min on ice. In the case of Jurkat cells, after the indicated time of stimulation, the Jurkat cells were recovered and lysed with lysis buffer (1% NP-40, 150 mM NaCl, 50 mM Tris, pH 7.4, 1 mM EDTA, 0.25% sodium deoxycholate, a protease inhibitor tablet (Roche Diagnostics, Mannheim, Germany)). Sodium dodecylsulfate polyacrylamide gel electrophoresis (SDS-PAGE), Western blotting, immunoprecipitations from the cell lysates were carried out as described (15). In vitro kinase assay for Raf-1 or B-Raf were carried out as described

below. Raf-1 and B-Raf were immunoprecipitated from cell lysates of T cells with the anti-Raf-1 and the anti-B-Raf antibodies, respectively. The immunoprecipitates were resuspended in 25 mM HEPES (pH 7.5), 10 mM $MgCl_2$, 10 mM □-glycerophosphate, 1 mM dithiothreitol, 10 □Ci [γ -^{32}P] ATP (Amersham Bioscience) and 0.8 □g recombinant GST-MEK protein. Reaction mixtures were incubated at 32 ℃ for 20 min, then the reactions were terminated by adding 5x SDS sample buffer, separated on 7% SDS-PAGE under the reducing condition, transferred to nitrocellulose membrane, and exposed to X-ray film. Relative amounts of MEK or ERK phosphorylation were calculated based on the ratio from the intensities of phospho-MEK or phospho-ERK bands to those of the whole MEK or ERK bands in whole cell lysates at each time point. Signal intensities of the bands were quantified by densitometric analysis using NIH Image 6.2 software. Nuclear extracts were prepared from B-Raf mutant- or mock-transfected TAg Jurkat cells for nuclear translocation analysis of NFAT using Nuclear / Cytosol Fractionation Kits (BioVision, CA).

7.6 Analyses of Ras and Rap activation

T5-32 ($1.0x10^7$) was co-cultured with the L cell transfectants and Jurkat cells stimulated with anti-CD3 antibody for the indicated time. Then they were lysed for 30 min in cold lysis buffer (1% NP-40, 20mM Tris, 200mM NaCl, 2.5mM $MgCl_2$, 1mM Na_3VO_4, 10% glycerol and a protease inhibitor tablet (Roche Diagnostics, Mannheim, Germany)). The supernatants after removing cell debris were mixed with the beads conjugated with GST-Ras binding domain of Raf (RBD) (Upstate Biothechnology) fusion protein, which selectively captures the GTP-bound form of Ras, and the mixture was gently rotated for 0.5-1 h at 4 ℃. In the case of the analyses of Rap activity, the beads conjugated with Rap binding domain of RalGDS-GST fusion protein that binds the GTP-bound form of Rap were used (57). The beads were washed with lysis buffer and solubilized in electrophoresis buffer (250 mM Tris pH 6.8, 8% SDS, 20% glycerol, 0.2% Bromophenol Blue, 8% 2-ME). Proteins were resolved in 12% sodium dodecylsulfate polyacrylamide gel electrophoresis (SDS-PAGE) and then blotted onto a nitrocellulose membrane. The activated Ras and Rap were detected by blotting with anti-K-Ras and anti-Rap antibodies, respectively.

7.7 Flow-cytometric analysis and cytokine measurement

For NFAT-GFP reporter assay, the TAg-Jurkat cells expressing B-Raf AA or mock vector were transfected with NFAT-GFP reporter construct and stimulated for 9 hr with immobilized anti-CD3 and anti-CD28 antibodies. The expression of GFP was analyzed with a flow-cytometer and CellQuest software (Becton-Dickinson). For intracellular staining, cells were fixed and permeabilized with IntraPrep (Immunotech, Marseille, France) and then stained with appropriate fluorescence-labeled antibodies. IL-2 concentrations in supernatants of T cell culture after 48 hr of stimulation were measured in an enzyme-linked immunosorbent assay (ELISA) using anti-human IL-2 antibodies.

7.8 Reverse transcriptase-polymerase chain reaction (RT-PCR)

Total RNA extraction and first-strand cDNA synthesis from T cells were done as described (58). The cDNA was subjected to polymerase chain reaction (PCR) amplification using sets of primers specific for human *B-Raf*: 5'-ACAACAGTTATTGGAATCTCTGG-3' and 5'-AAATGCTAAGGTGAAAAACG-3', or mouse *B-Raf*: 5'-CCATTCGCCACCCAAGTTGG-3' and 5'-CTGGTGCAGCAGAGCTTTCC-3', respectively.

7.9 Luciferase assay

Reporter constructs were transfected into the Jurkat cells expressing wild-type or mutant B-Raf. A β-galactosidase expression plasmid was co-transfected to normalize the variations in transfection efficiency. After 24 hr of transfection, cells were harvested and stimulated. Luciferase assay was carried out according to the protocol in the Pica Gene kit (Toyo Ink, Tokyo, Japan). β-galactosidase expression was assessed using the Luminescent β-galactosidase detection kit II (Clontech, Palo Alto, CA) according to the manufacturer's instruction.

7.10 Preparation of lentiviral vectors and infection to T cells

The packaging construct pCAG-HIVgp, VSV-G- and Rev-expressing construct, pCMV-VSV-G-RSV-Rev, and self inactivating (SIN) vector construct, CS-RfA-EG that contains the (enhanced green fluorescent protein) EGFP gene under the control of EF-1a promoter, were provided from H. Miyoshi. To express the B-Raf wild type (WT) or S598/601A (AA) in T5-32, hemagglutinin-tagged B-Raf WT or AA (51) was inserted into the cloning site in SIN vector. The synthesized complementary oligonucleotide containing the target sequence for small hairpin (sh)RNA against human B-Raf was inserted into the shRNA expression vector (pSilencer 3.0, Ambion Inc). Next, the expression cassette of human U6 promoter-driven shRNA for human B-Raf or luciferase mRNA was subcloned from the vector and ligated into the SIN vector. The target sequences for shRNA against luciferase (irrelevant control) and human B-Raf were 5'-CGTACGCGGAATACTTCGA-3' and 5'-GGTGTGGAGTTACAGTCCG-3', respectively. For the preparation of lentiviral vectors, 293T cells were transiently co-transfected with the recombinant SIN vector construct, pCAG-HIVgp, and pCMV-VSV-G-RSV-Rev using lipofectAMINE 2000 reagent (Invitrogen) according to the manufactures' instruction. The virus-containing supernatants were collected 72 h after transfection and then were concentrated by ultracentrifugation at 25,000 g for 2 h. The virus precipitates were resuspended with a small amount of RPMI medium. For infection, T5-32 (1x 10^5) was cultured in RPMI medium supplemented with 20% FCS and virus solution in 96-well U-bottom plates. After 72 h of incubation, the T cells were harvested and stimulated with indicated L cells.

8. Results

8.1 Q59G/HLA-DR4 complexes provide relatively low-avidity TCR ligand for T5-32 as compared with M12/HLA-DR4 complexes

To characterize the precise signaling pathway(s) underlying the interactions of specific TCR-APL/HLA complex in human T cells, it was necessary to obtain a large number of a monoclonal T cell clone. To overcome this problem, we applied HVS to the human $CD4^+$ T cell clone, YN5-32, in order to transform the T cell clone. Human T cells immortalized by HVS infection have been reported to preserve their intact T cell responses to cognate antigens (55). As previously reported, established HVS-transformed T5-32 exhibited IL-2-dependent proliferation without periodical antigen stimulation ((55) and data not shown). As observed in parental cell clone, YN5-32, the cognate stimulation with agonistic peptide, M12/HLA-DR4 complexes provoked the proliferation of T5-32 in a peptide dose-dependent manner (Fig. 7A). On the other hand, some antagonistic peptides with a amino acid substitution in the M12 peptide suppressed the agonistic stimulation-induced proliferation of T5-32 (Fig. 7B). These results provided the compelling evidence that T5-32 retained the responsiveness toward the antigen, including antagonistic peptide that was identical to that of YN5-32.

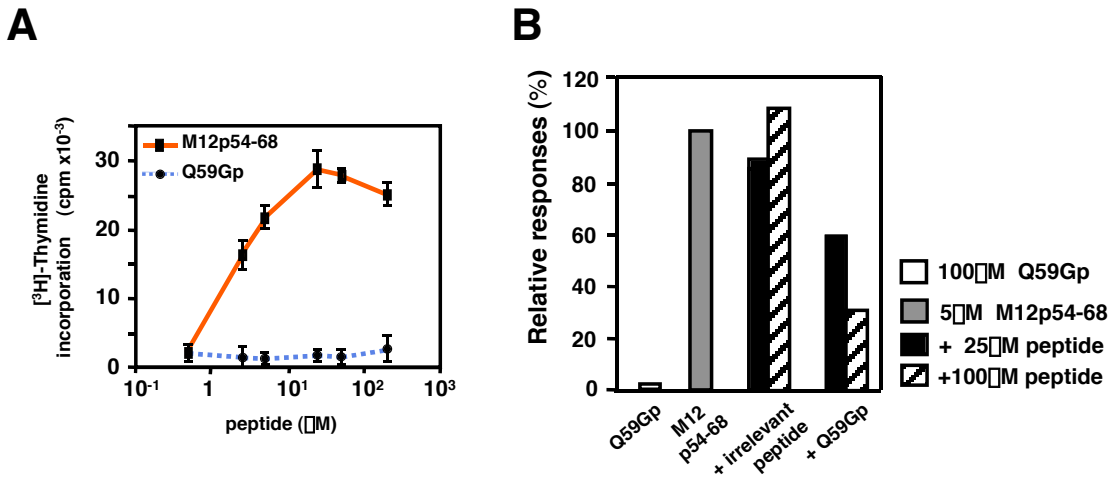

Fig. 7 Q59G peptide is relatively low affinity ligand for cognate TCR.

A, T5-32 were stimulated with L-DR4 cells pulsed with M12p54-68 or Q59G peptide (Q59Gp) at the indicated concentrations. The proliferation of T5-32 was determined by [^{3}H] thymidine incorporation.

B, L-DR4 were pre-pulsed with 5 μM M12p54-68. After washing, L-DR4 was incubated with additional Q59G or irrelevant peptides (25 μM; black bars, 100 μM; shaded bars). T5-32 were then co-culured with L cells, and proliferation was determined by [^{3}H] thymidine incorporation. A gray bar shows the T cell proliferative response stimulated with 5 μM M12p54-68 in the absence of analogue peptide and this response of T5-32 was represented as 100%. Each relative response was calculated from the proliferative responses of T5-32 stimulated with the indicated conditions.

We took advantage of a system in which a series of L cell transfectants expressing APLs covalently linked to HLA-DR4 molecules were employed as APC to present the APL/HLA complexes at various density to T5-32 (8,15,19). Consistent with the results in YN5-32 (22), T5-32 proliferated vigorously in recognition of M12/HLA-DR4 complexes expressed on L cells (the high-avidity interactions). The proliferative response reached plateau level at the density of 1-5 x10^5 ligand /L cell (Fig. 5B). In contrast to the high-avidity interactions, at similar density, little proliferative response was provoked by stimulation with Q59G/HLA-DR4 complexes expressed on L cells (the low-avidity interactions) presenting a peptide with a substitution from glutamine to glycine at position 59 of the M12 peptide (8). In proportion to increasing the ligand density, proliferation stimulated with Q59G/HLA-DR4 complexes was augmented. However, the threshold of ligand density required to induce substantial proliferation was much higher than that of M12/HLA-DR4 complexes (Fig. 5B). This is due to the lower affinity of the Q59G/HLA-DR4 complex toward TCR as compared with that of the M12/HLA-DR4 complex. We refer to the L cell clones expressing each peptide/HLA-DR4 complex that induced a maximal response of T5-32 as M12DR4 and Q59GDR4, respectively. As observed in YN5-32, L cell expressing another antagonistic APL, Y61VDR4 never provoked the T cell proliferation even at a similar ligand density (22 and Fig. 5B). These data excluded the possibility that Q59GDR4-induced T cell proliferation was due to the recognition of the artificial or unknown peptide bound-HLA-DR4 molecules. The conservation of ligand specificities in T5-32 allowed us to explore the specific TCR-mediated intracellular signaling stimulated by the TCR engagement with different avidities.

8.2 Alternative TCR-mediated signals induced by stimulation with Q59GDR4

We next analyzed the delineating differences in TCR-mediated intracellular

signaling between the stimulation with M12DR4 and Q59GDR4 regarding their avidity toward TCR. As shown in Fig. 8A, tyrosine phosphorylation of ZAP-70/LAT/SLP-76 were induced by M12DR4 at 5 min and thereafter gradually declined as time went by. On the other hand, the pattern of tyrosine phosphorylation induced by Q59GDR4 was similar to those in non-stimulated or Y61VDR4-stimulated T cells. T cells stimulated with Q59GDR4 as well as Y61VDR4 were refractory to phosphorylation of these molecules throughout the analysis period (0-60 min). These observations indicated that the T cell proliferation depended on the density of the Q59G/HLA-DR4 complex, while the tyrosine phosphorylation of ZAP-70/LAT/SLP-76 did not.

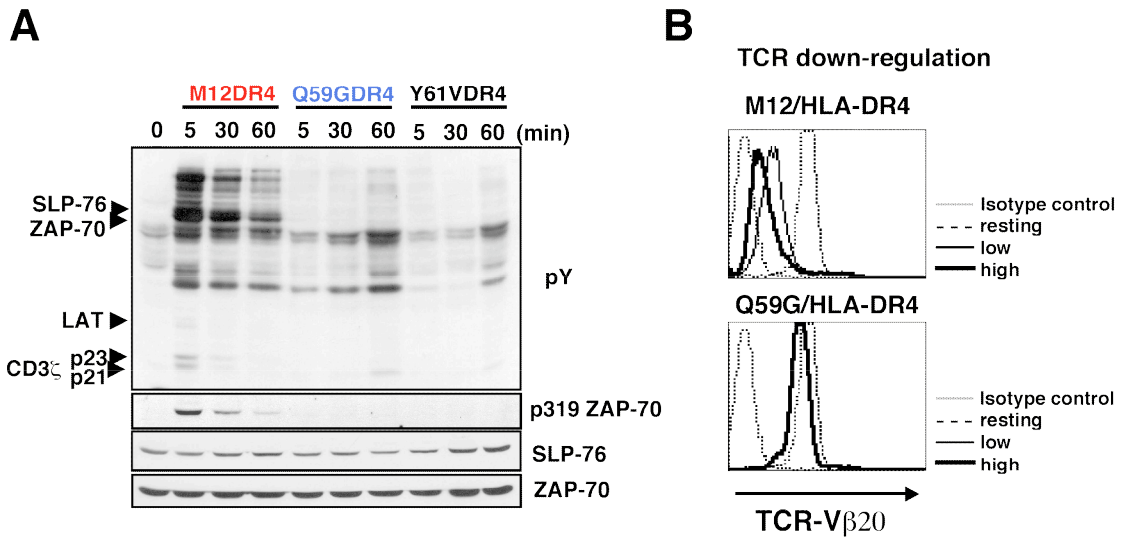

Fig. 8 Q59GDR4 stimulation exhibited the characteristics of low avidity TCR ligand. A, T5-32 was stimulated with M12DR4 or its variants for the indicated times. Their whole cell lysates were analyzed by immunoblotting for phosphotyrosine (pY) and phospho-Y319-ZAP-70 (p319 ZAP-70). Blotting for total SLP-76 and ZAP-70 shows equal protein loading between each lane. The results were representative of three experiments with similar results. B, T5-32 were stimulated with L cells expressing high or low density of M12/HLA-DR4 complexes or its variants indicated in Fig. 5B for 6 hr. Their TCR expressions were assessed by flow cytometric analyses.

The high avidity stimulation induces TCR-down regulation from its cell surface, whereas the low avidity stimulation does not induce (#). Induction of TCR down

regulation is thought to be correlated with proliferative response of T cells. However, Q59GDR4 stimulation failed to down regulate the TCR, which is representative feature observed in T cells stimulated with low avidity TCR interaction (Fig. 8B).

Since tyrosine phosphorylation of ZAP-70/LAT/SLP-76 molecules are believed to be located up-stream of the Ras/ERK pathway (59-61), we examined whether the Ras/ERK pathway was activated with Q59GDR4 stimulation. As shown in Fig. 9A, both the stimulation with M12DR4 and Q59GDR4 induced the up-regulation of CD69, which is a T cell activation marker dependent on TCR- and Ras/ERK-mediated pathway (23). Next, we directly analyzed the Ras activation in response to M12DR4 or Q59GDR4 stimulation. Concomitant with the up-regulation of CD69, Ras activation started within 5 min and lasted at least for 30 min in both M12DR4 and Q59GDR4 stimulations (Fig. 9B). In addition to Ras, we also estimated the activity of Rap1, another small GTPase expressed in T cells, in both stimulatory conditions because it was previously reported that Rap1 activity integrates and modulates the Ras/ERK activation events (62). In these experiments, Rap1 activity was also up-regulated in both M12DR4 and Q59GDR4 stimulations for 60 min after TCR engagement (Fig. 9C). These data demonstrated that Ras and the Ras modulator, Rap1 were equally activated in both stimulatory conditions, whereas Rap activation appeared to be more sustained than Ras activation. We further examined the dependency of ERK activation in Q59GDR4-induced T cell activation using a specific inhibitor of MEK/ERK pathway, U0126. The U0126 treatment markedly reduced the IL-2 production and proliferation in response to both M12DR4 and Q59GDR4 (Fig. 9D and data not shown). Thus, these results suggested that the Ras/ERK activation cascade comparably contributed to T cell activation induced by both stimuli.

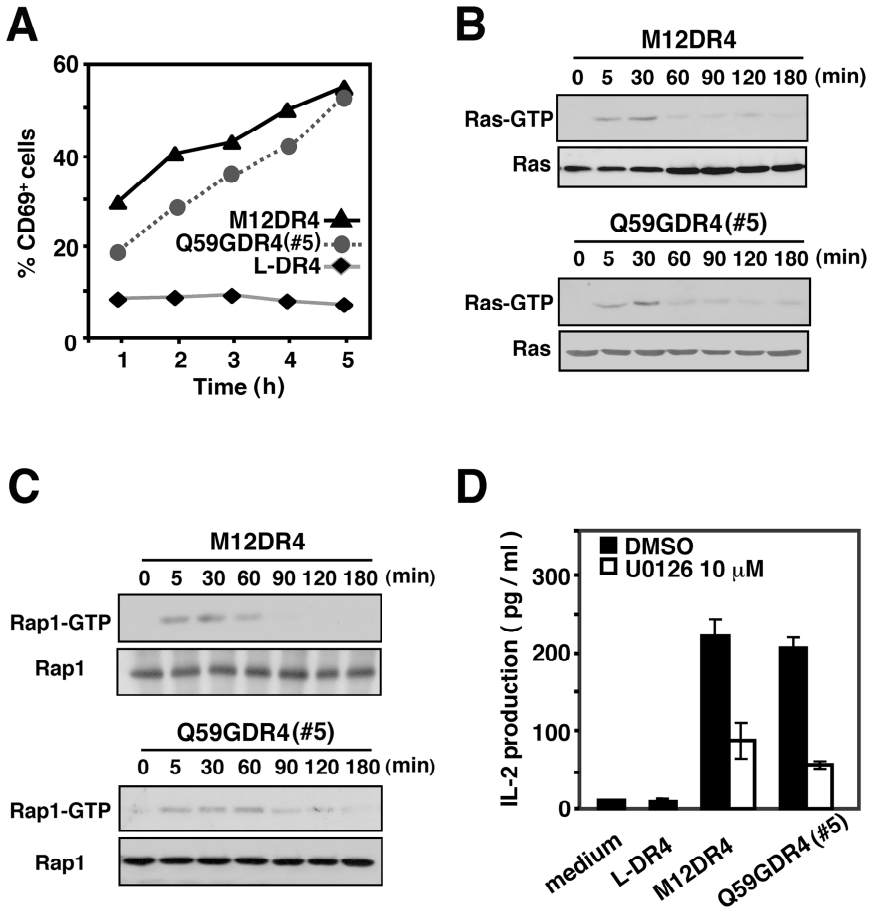

Fig. 9 Ras/ERK pathway was activated by both M12DR4 and Q59GDR4 stimulation. A, T5-32 was co-cultured with the each L cells for indicated time and CD69 expression was measured by flow cytometry. The percentage of CD69 positive cells in all $CD4^+$ cells is shown. B, T5-32 was stimulated with M12DR4 or Q59GDR4 (#5) for the indicated times. The cell lysates were then subjected to pull-down assays with Raf1-RBD-Sepharose followed by SDS-PAGE and immunoblotting with an anti-Ras antibody to detect GTP-bound Ras (upper panels). The existence of whole Ras protein at a comparable level in each T cell was confirmed (lower panels). C, Rap1 activity was estimated by pull-down assays with RalGDS-RBD-Sepharose as described in B. The comparable level of Rap1 protein in each condition was indicated in lower panels. D, T5-32 was pretreated with DMSO (black bars) or 10 □M U0126 dissolved in DMSO (white bars) for 30 min. Each T cells were then stimulated with M12DR4 or Q59GDR4 (#5). The IL-2 production in each cell culture for 36 h was determined by ELISA. All values are means ± SD.

8.3 TCR engagement with Q59GDR4 resulted in a delayed and sustained activation of ERK

We directly asked whether MEK/ERK activation could occur following Q59GDR4 stimulation. T5-32 stimulated with M12DR4 led to a detectable MEK activation, which rapidly reached to a plateau level within 5-10 min and returned to baseline levels within 5-7 h (early and late phase, respectively, upper panels of Fig. 10A). On the other hand, to our surprise, Q59GDR4 stimulation resulted in no detectable MEK activation until 30 min, and the gradual accumulation of phospho-MEK at 60 min (early phase, upper panels of Fig. 10A). The signal intensity of Q59GDR4-induced MEK activation reached to maximal level at 2-3 h after TCR ligation, but the magnitude of activation was smaller than that induced by M12DR4. The MEK activation was sustained as long as for 7 h (late phase, upper panels of Fig. 10A). Parallel results were obtained in ERK activation (lower panels of Fig. 10A), implying the direct consequence of MEK activation on ERK regulations. Fig. 10B gives a summary for kinetics of ERK phosphorylation stimulated with M12DR4 or Q59GDR4. These findings suggested that Q59GDR4 exerted a delayed and sustained ERK activity than that observed in M12DR4-stimulated T cells.

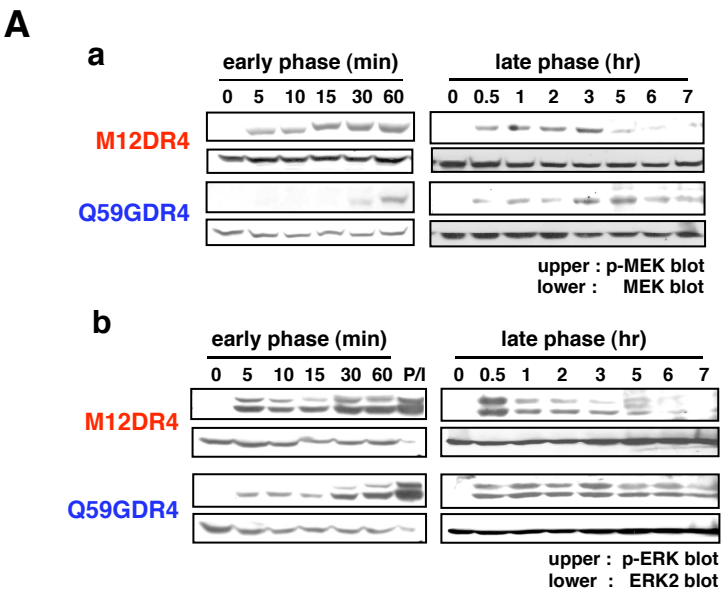

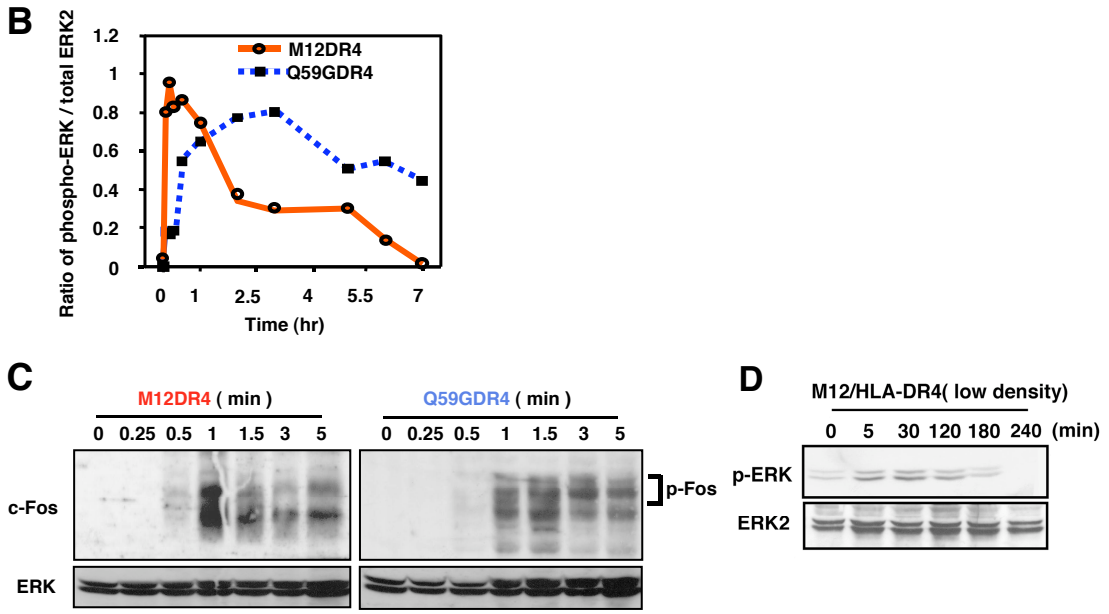

Fig. 10 The differential kinetics of MEK/ERK phosphorylation between M12DR4- and Q59GDR4-stimulated T cells. A, T5-32 was co-cultured with M12DR4 or Q59GDR4 (#5) for the indicated times (early and late phase). The cell lysates were subjected to SDS-PAGE, and the blot was probed with anti-phospho-MEK specific antibodies (A, upper panels) and anti-phospho-ERK specific antibodies (A, lower panels). PMA and ionomycin stimulation (P/I) for 10 min was a positive control of ERK phosphorylation. Essentially similar results were obtained in three independent experiments. B, The intensity of the ERK phosphorylation in M12DR4 (bold line)- or Q59GDR4 (#5) (dotted line)-stimulated T cells was quantified by densitometric analyses. The plot showed the ratio of phospho-ERK/total ERK as a parameter of ERK activity based on a mean ratio of the phospho-ERK to total ERK2 signal intensities at each time point. The data were normalized to the densitometric values of their respective loading controls and to the relative activation level in unstimulated cells (at zero time point). Values are means ± SD. C, T5-32 were stimulated with M12DR4 or Q59GDR4 (#5) for the indicated times. Whole cell lysates were analyzed by immunoblotting for c-Fos protein and ERK to show equal loading. D, T5-32 was stimulated with L cells expressing M12/HLA-DR4 complexes at a relatively low density (~1x10^5/cell) described in Fig. 1A for the indicated times. Each sample were analyzed as described in Fig. 3A.

The c-Fos transcription factor is known to be phosphorylated by activated ERK, resulting in an increased stability of the c-Fos protein (63). We expected that the kinetics of MEK/ERK activation in Q59GDR4-stimulated T5-32 would affect the expression and phosphorylation of c-Fos. Consistent with this expectation, Q59GDR4-induced accumulation and phosphorylation of c-Fos were weak, retarded and sustained as compared with those observed in M12DR4-stimulated T cells (Fig. 10C).

Similar to the case of M12DR4 stimulation, ERK was immediately activated at 5 min after stimulation and, this activation gradually declined after 3 h of stimulation even in T5-32 exposed to L cell expressing M12/HLA-DR4 complexes at a minimal density (1 x10^5/L cell) in Fig. 5B (Fig. 10D) or HLA-DR4 molecule loaded with sub-optimal dose (5 μM) of M12p54-68 peptide, which induced weak but not maximal proliferation (data not shown). Given that the stimulation with the agonist at relatively lower density did not induce a retarded ERK activation, it may not be likely that the stimulation with a high density of the APL transmitted a merely weaker signal than did the agonist. Therefore, it appeared possible that the kinetic pattern of Q59GDR4-induced ERK activation was regulated by mechanisms qualitatively distinct from that induced with M12DR4.

8.4 Q59GDR4 stimulation provokes B-Raf but not Raf-1 activation

The ERK activation cascade consisting of Ras, Raf-1, MEK and ERK plays crucial roles in the intracellular signals inducing IL-2 production and T cell proliferation (59,64,65). Hence, we evaluated whether M12DR4 and Q59GDR4 stimulation induced Raf-1 activation. The activation of Raf-1 requires the phosphorylation of Raf-1 at serine 338 and tyrosine 340/341 (66). As shown in Fig. 11A, as expected, the immediate and transient phosphorylation at these residues of Raf-1 were observed in response to M12DR4 stimulation. In marked contrast, when T5-32 was stimulated with Q59GDR4, the phosphorylation of Raf-1 was never induced throughout the analysis period (Fig. 11A, right panels). To confirm their phosphorylation status, we also investigated the kinase activity of Raf-1 by in vitro kinase assay (Fig. 11B). Concomitant with their phosphorylation, M12DR4 stimulation provoked the up-regulation of kinase activity of Raf-1. On the other hand, upon Q59GDR4 stimulation, the kinase activation of Raf-1 was not observed at all. It was thus concluded that Raf-1 activation could not be induced by stimulation with excessively increased density of Q59G/HLA-DR4 complex even if the stimulus was sufficient to elicit a substantial magnitude of T cell proliferation.

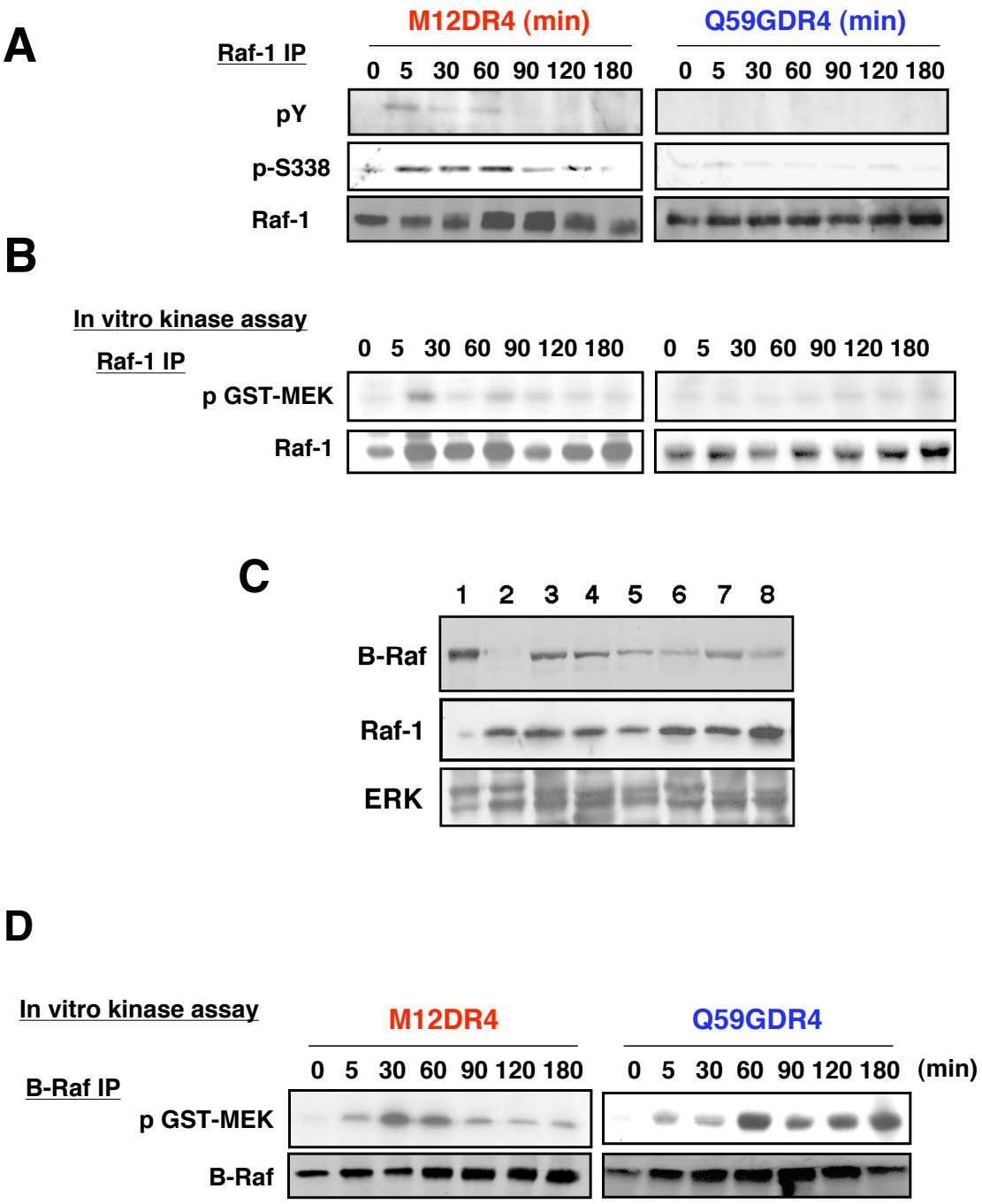

Fig. 11 B-Raf but not Raf-1 was activated by the Q59GDR4 stimulation.

A. T5-32 was stimulated as described in Fig. 3. Immunoprecipitates (IP) with anti-Raf-1 antibodies from T5-32 stimulated with M12DR4 (left panels) or Q59GDR4 (#5) (right panels) for the indicated time were subjected to SDS-PAGE and blotting with anti-phosphotyrosine (pY) (upper panels), anti-phospho-Raf-1 (Ser 338 specific) (middle panels) and an anti-Raf 1 antibody (lower panels) for comparable loading control. These results shown herein were representative of three independent and reproducible experiments. B, In vitro kinase assays for Raf-1 isolated from T cells stimulated in each condition.

Recombinant GST-MEK was used as a substrate and incorporated ^{32}P radioactivities were visualized by autoradiography (upper panels). Equal loading of Raf-1 protein was confirmed by blotting with an anti-Raf-1 antibody (lower panels). C, Western blotting analysis for B-Raf expression in various T cells. Lane 1, PC12 cells; lane 2, NIH3T3 cells; lane 3, Jurkat cells; lane 4, primary human $CD4^+$ T cells; lane 5, T5-32; lane 6, primary mouse $CD4^+$ T cells; lane 7, T5-32 expressing shRNA for luciferase; lane 8, T5-32 expressing shRNA for human B-Raf. Raf-1 and ERK blottings were used as loading control. D. In vitro kinase assays for B-Raf were performed as described in Fig.4 B. Equal loading of B-Raf protein was confirmed by blotting with an anti-B-Raf antibody (lower panels).

Although the tyrosine phosphorylation of the TCR proximal signaling molecules including Raf-1 were not detected when stimulated with Q59GDR4, MEK/ERK activation actually occurred. These seemingly discrepancies prompted us to speculate the other molecule responsible for MEK/ERK activation in the Q59GDR4-stimulated T5-32. The one of most likely candidate is B-Raf, another Raf family molecule since B-Raf is strong activator of MEK (67). To evaluate the expression of B-Raf in T cells, we utilized RT-PCR to detect RNA transcripts of B-Raf. Murine T cell line expressed the mRNA from *b-raf* gene (data not shown). We next compared the expression level of B-Raf protein in T cells including T5-32, and used PC12 cells and NIH3T3 cells as positive and negative control, respectively (68). B-Raf was expressed in T5-32 as well as in human primary $CD4^+$ T cells and the expression level of B-Raf in both cells were comparable (Fig. 11C). These results indicated that T5-32 represents normal human $CD4^+$ T cells in terms of B-Raf expression. As compared to human T cells, B-Raf expression in murine T cells was smaller. Moreover, the decrease of the B-Raf expression in T5-32 by the RNA interference with B-Raf-targeted shRNA confirmed the specificity of B-Raf expression. This shRNA expression does not abolish the Raf-1 expression. We thus conclude that B-Raf is expressed in both human and mouse T cells, allowing us to examine B-Raf functions in TCR-mediated T cell activation. Based on the results, B-Raf can be the possible candidate of MEK/ERK activator in Q59GDR4-stimulated T cells. Hence, we next assessed the status of B-Raf activation under each stimulatory condition. M12DR4-stimulated T cells exhibited a prominent activation of B-Raf, which was maximal at 15 min and then declined at 60 min after TCR engagement (Fig. 11D, left panels). Compared with M12DR4 stimulation, Q59GDR4 stimulation induced much gradual and sustained B-Raf activation, especially after 60 min of stimulation (Fig. 11D, right panels). In both stimulatory conditions, the

kinetics of B-Raf activation closely coincided with those of ERK activation. Taken together, these results suggested that Q59GDR4-induced MEK/ERK activation was less dependent on the Raf-1 activity and that Raf-1 selectively contributes to rapid MEK/ERK activation in M12DR4-stimulated T cells, and that B-Raf activity regulated the retarded MEK/ERK activity induced by the Q59GDR4 stimulation.

8.5 B-Raf activation has a lower threshold than Raf-1 activation does

Our observations raised the question why B-Raf was selectively activated by the stimulation with Q59GDR4. One possible explanation is that B-Raf may have higher sensitivity than Raf-1 does for TCR-mediated relatively weaker signal. We analyzed the ability of the crosslinking of the CD3 complex with various concentrations of anti-CD3 mAb to activate each kinase in human T cell line, Jurkat, because this allows us to determine whether there are any intrinsic biochemical differences in the activation thresholds between the two Raf kinases activated by the same stimulus. As shown in Fig. 12A, Raf-1 was completely inactive, while B-Raf was only slightly active even in T cells without stimulation. Following stimulation for 5 min, 0.125 □g/ml of anti-CD3 mAb was enough to provoke the plateau level of B-Raf and ERK activation. However, a maximal Raf-1 activation was not achieved by the stimulation at the same concentration of antibody. The anti-CD3 mAb dose required for maximal activation of B-Raf was about 0.10 □g/ml. On the other hand, that of Raf-1 was 0.25 □g/ml, a twofold higher concentration than B-Raf (Fig. 12B). These data suggest that B-Raf activation is more sensitive to relatively weak TCR stimulation and that B-Raf exhibited a lower activation threshold than Raf-1 did in T cells.

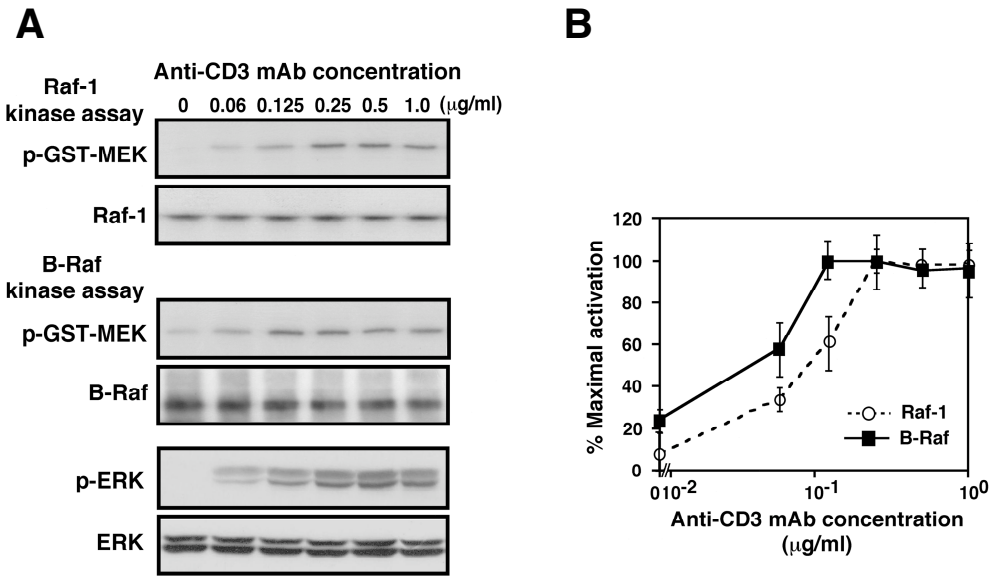

Fig. 12 The differential sensitivity of Raf kinases activation to the magnitude of TCR stimulation. A, Jurkat T cells were kept unstimulated or stimulated for 5 min by crosslinking with different concentrations of anti-CD3 antibody followed by the addition of anti-mouse Ig antibody. In vitro kinase assays for Raf-1 and B-Raf were performed by measuring the incorporations of ^{32}P radioisotope into recombinant GST-MEK as a substrate for Raf kinases. Immunoprecipitated Raf kinases were revealed by Western blot analyses. For ERK activation, total cellular proteins were separated on SDS-PAGE and revealed by blotting using an anti-phospho-p42/44 ERK antibody and reprobed with anti-ERK antibody. B, The right panel represents the percentage of each Raf kinases activities in each condition of stimulation when maximal activity is assigned to be 100%. The relative value was normalized by calculating the percentage of GST-MEK phosphorylation intensity as compared with that of immunoprecipitated protein at each stimulatory condition. Values represent the means ± SD from three independent experiments.

8.6 Correlation between B-Raf/ERK pathway activation, TCR ligand avidity and T cell proliferation

We favor the idea that the selective activation of B-Raf due to its high sensitivity to TCR stimulation contributes to T cell activation in response to Q59GDR4. Since the increased density of Q59G/HLA-DR4 complex correlated with larger proliferative response of T cells (Fig. 5B), it seemed possible that the TCR ligand avidity may directly influence the state of B-Raf activation in T cells stimulated with the low-avidity TCR ligand. To test this hypothesis, we employed L cell transfectants expressing various levels of Q59G/HLA-DR4 complexes as APC (Fig. 5B). As shown in Fig. 6A, very weak B-Raf activation was observed in T cells stimulated even with L cells

expressing Q59G/HLA-DR4 complexes at the lowest density (clone #1), which hardly elicits any proliferation of T cells. Furthermore, other L cell clone #4 and, to a lesser extent, clone #2 induced B-Raf activity at 2-3 h after TCR engagement. As the density increased, so did the level of B-Raf activity (Fig. 13A). We next examined the correlation between the density of Q59G/HLA-DR4 complexes and ERK activity under such stimulatory conditions. The ERK activation was very weak and transient upon stimulation with the L cell clones #1 and #2 expressing Q59G/HLA-DR4 complex at relatively low density (Fig. 5B). In contrast, stimulation at a high density by L cell clones #3 and #4 that provoked reliable T cell proliferation resulted in strong and prolonged ERK activation (Fig. 13B). The increased density of Q59G/HLA-DR4 complexes on APC was closely correlated with the prolongation and augmentation of B-Raf/ERK activity in T cells. These results thus suggest that TCR-mediated B-Raf and ERK activation is indeed determined by both the quality and the density of the TCR ligand (TCR ligand avidity).

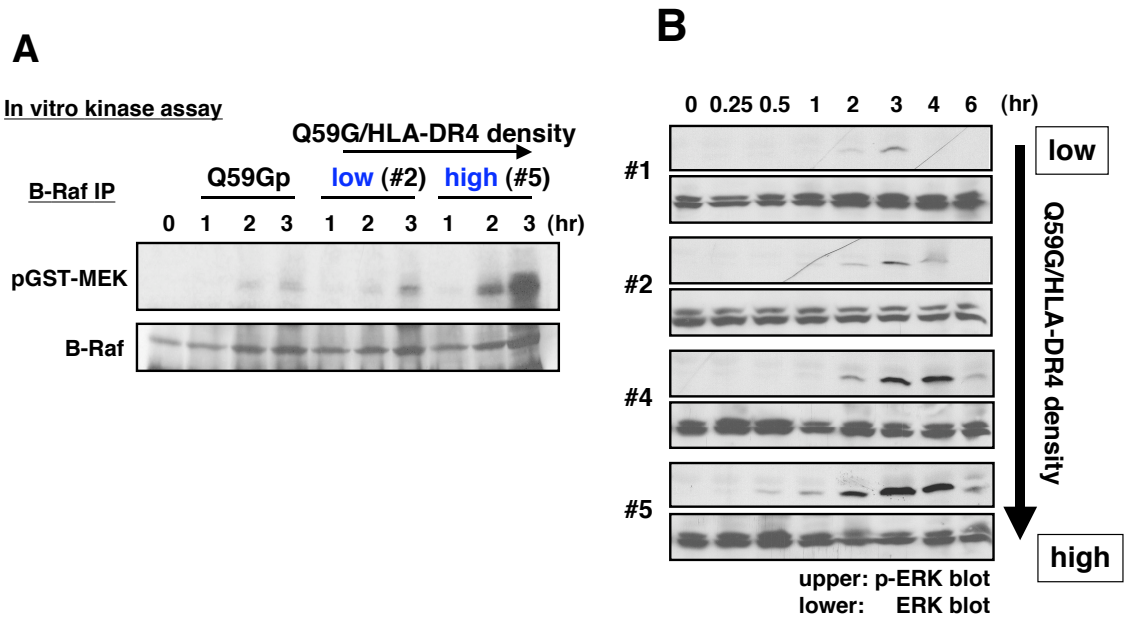

Fig. 13 B-Raf/ERK activation was sensitive to the density of Q59G/HLA-DR4 complexes. A, T5-32 was stimulated with L cell clones expressing Q59G/HLA-DR4 complexes at various density (#1, #2 or #4 as described in Fig. 5B) for the indicated time. In vitro kinase assays for B-Raf were performed as in Fig. 4C. Blotting with anti-B-Raf antibody indicated equal protein loading (lower panel). B, ERK activation profiles of T5-32 stimulated with L cell clones (#1-4) expressing

Q59G peptide/HLA-DR4 complexes. The upper and lower panels show phospho-ERK and total ERK, respectively. Each result from three independent experiments was essentially the similar and a representative one is shown. IP: immunoprecipitation

8.7 B-Raf plays an indispensable role in both agonist and APL/HLA complex-induced T cell activation

Given the possibility that relative activity of B-Raf depending on TCR-mediated stimulation sensitive to the density of Q59G/HLA-DR4 complex affects the T cell activation, we investigated whether B-Raf activity was indeed responsible for those responses. The lentivirus vector was utilized to transduce and express a dominant negative form of B-Raf (B-Raf AA) which Thr 598 and Ser 601 were substituted to Ala (Fig. 6 and Ref. 33) into T5-32 to interfere with endogenous B-Raf but not Raf-1 activity (51,56). Polycistronic vector co-expressing GFP and B-Raf AA allowed us to monitor the B-Raf expression by detecting the GFP fluorescence intensity (69). Using this experimental system, we first analyzed the effect of B-Raf on ERK activation induced by either M12DR4 or Q59GDR4 stimulation in mock- and B-Raf AA-transduced T5-32. As shown in Fig. 14A, in mock-transfected GFP^+ T5-32, M12DR4 and Q59GDR4 stimulation induced the comparable degree of ERK phosphorylation (M12DR4: 98%, Q59GDR4; 83%), as compared to GFP^- T5-32. On the other hand, M12DR4-induced_ERK phosphorylation was merely inhibited ($p\text{-}ERK^+$ in GFP^+ fraction; 54%), and ERK activations induced by Q59GDR4 were more severely suppressed in B-Raf AA expressing T5-32 ($p\text{-}ERK^+$ in GFP^+ fraction; 13%), but not in GFP^- counterparts. For further confirmation, western blotting analyses of MEK/ERK phosphorylation were performed (Fig. 14B). M12DR4-induced MEK/ERK phosphorylation was slightly inhibited by B-Raf AA expression, while Q59GDR4-induced MEK/ERK phosphorylation was markedly suppressed.

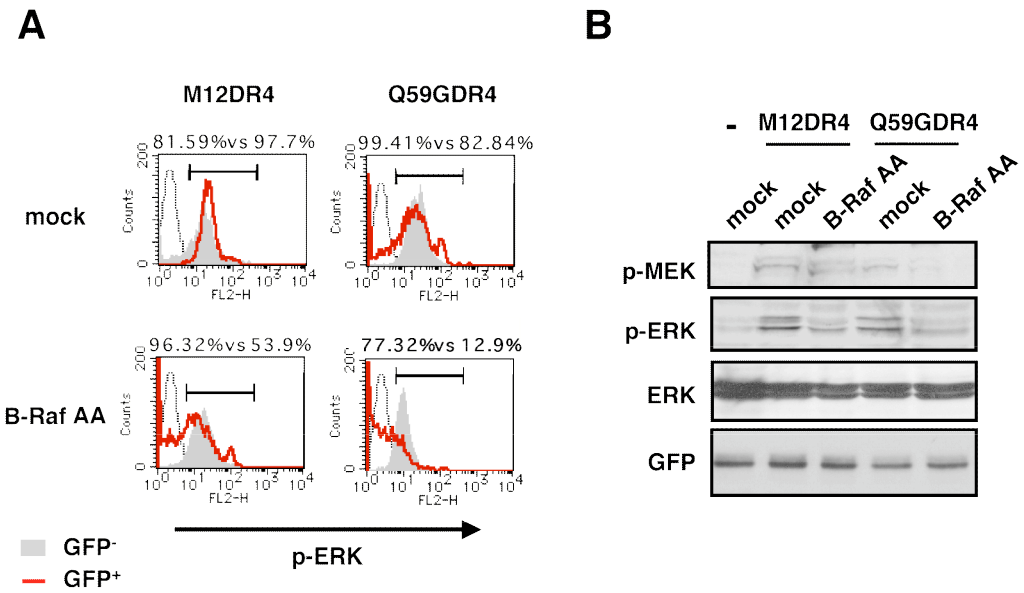
A
M12DR4
Q59GDR4
mock
B-Raf AA
81.59%vs 97.7%
99.41%vs 82.84%
96.32%vs 53.9%
77.32%vs 12.9%
Counts
FL2-H
GFP-
GFP+
p-ERK
B
-
M12DR4
Q59GDR4
mock
mock
B-Raf AA
mock
B-Raf AA
p-MEK
p-ERK
ERK
GFP

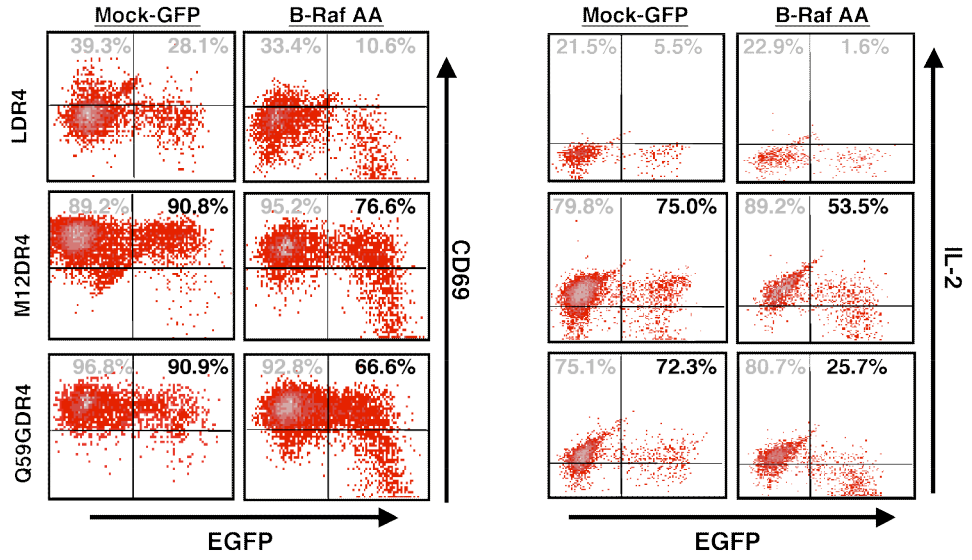
C
Mock-GFP
B-Raf AA
LDR4
M12DR4
Q59GDR4
39.3%
28.1%
33.4%
10.6%
89.2%
90.8%
95.2%
76.6%
96.8%
90.9%
92.8%
66.6%
CD69
EGFP
D
Mock-GFP
B-Raf AA
21.5%
5.5%
22.9%
1.6%
79.8%
75.0%
89.2%
53.5%
75.1%
72.3%
80.7%
25.7%
IL-2
EGFP

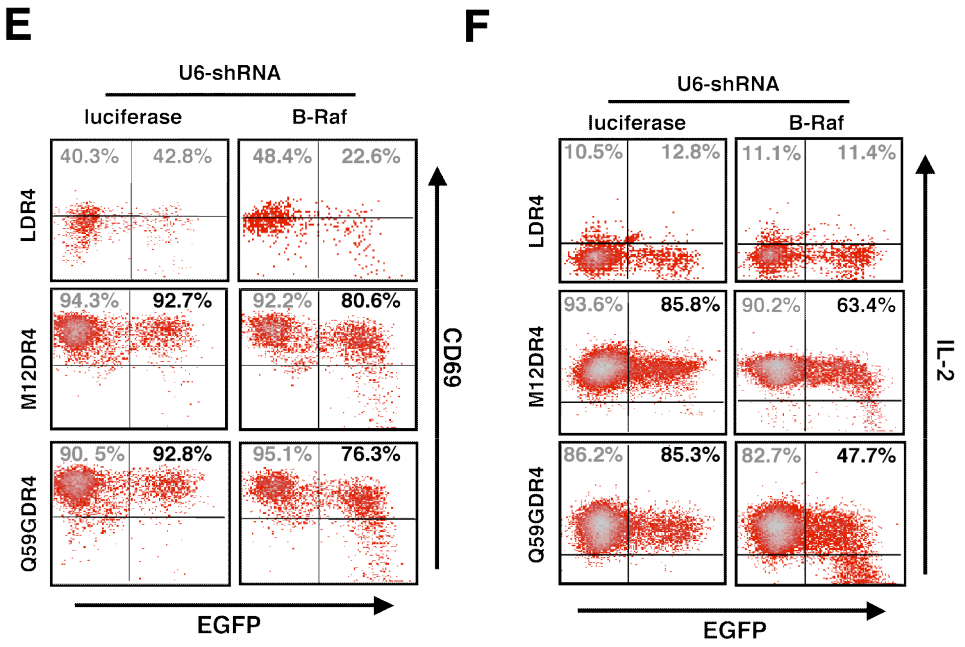

Fig. 14 Abrogation of B-Raf activity markedly attenuated the T cell activation stimulated by Q59GDR4.

A, T5-32 expressing mock-GFP or B-Raf AA were stimulated with M12DR4 or Q59GDR4 (#5) for 2 h. The cells were then stained intracellularly for phospho-ERK. The histograms show the levels of ERK phosphorylation in GFP^- (shaded) or GFP^+ (thick line) fraction in T cells transfected with mock-GFP (upper panels) or B-Raf AA (lower panels) stimulated with M12DR4 (left panels) or Q59GDR4 (#5) (right panels). The dotted lines indicate the levels in the cells co-cultured with L-DR4 as negative control. B, MEK and ERK activation in T5-32 expressing mock-GFP or B-Raf AA stimulated with indicated L cells were estimated by western blotting analysis. Approximately 50 % of T cells in each condition were GFP positive. GFP expression confirmed the successful transfection in each cells. C, D, E and F, T5-32 expressing mock-GFP, B-Raf AA (C, D), shRNA for luciferase or human B-Raf (E, F) were stimulated with M12DR4 or Q59GDR4 (#5), and $CD69^+$ (C, E) or IL-2 producing (D, F) cells were enumerated. The data are displayed as two-color density plots showing GFP (horizontal axis) versus CD69 expression or IL-2 secretion (vertical axis). The percentage shown in each column independently indicates the percentages of positive cells in each GFP^- or GFP^+ fraction. The typical representative data from three reproducible experiments are shown.

We next evaluated the up-regulation of CD69 in response to either M12DR4 or Q59GDR4 stimulation in T cells expressing B-Raf AA. As shown in Fig. 14C, similar to GFP^- fraction, the frequency of $CD69^+$ cells in the GFP^+ fraction increased in response to M12/DR4 stimulation (from 28% to 91%; upper right quadrants) when mock-GFP was transduced. On the other hand, the expression of B-Raf AA mildly reduced the frequency of $CD69^+$ cells in the GFP^+ population from 91% to 77%

compared with those in GFP^- fraction (from 89% to 95%). Furthermore, in the case of Q59GDR4 stimulation, we could also detect the effects of B-Raf AA on induction of $CD69^+$ cells since an analysis of GFP^+ $CD69^+$ cells revealed a B-Raf AA-induced reduction of $CD69^+$ cells in a representative experiment (mock-GFP; 91%, AA; 67%). Notably, these reductions were pronounced in T cells with increasing GFP intensity.

Finally, we examined whether attenuation of B-Raf activity negatively influence the IL-2 production in T5-32 (Fig. 14D). As a control, GFP^+ T cells expressing mock-GFP produced IL-2 in response to M12DR4 (75%) or Q59GDR4 (72%). In contrast to mock-GFP-infected cells, compared with GFP^- cells, IL-2 producing cells in B-Raf AA expressing GFP^+ fraction were reduced in M12DR4-stimulated condition ($IL\text{-}2^+$ in GFP^+ fraction; 54%). This is consistent with previous results that B-Raf AA expression prevented Jurkat cells from leading full IL-2 production in response to TCR stimulation (56). On the other hand, the Q59GDR4-stimulated IL-2 production was severely compromised as B-Raf AA (GFP) expression increased ($IL\text{-}2^+$ in GFP^+ fraction; 26%). Basically identical results were also obtained by knockdown of B-Raf expression with RNA interference approach using lenticvirus vector expressing shRNA specific to human B-Raf (Fig. 11C and Fig. 14E, F), confirming the specific role of B-Raf in regulation of Q59GDR4-stimulated T cell activation. It is noteworthy that these inhibitory effects were more prominent in Q59GDR4 stimulated T cells, implying that dependency on B-Raf activity of these responses induced by Q59GDR4 was much higher than that induced by M12DR4. Collectively, it was directly indicated that the B-Raf/ERK pathway plays a crucial role in the low-avidity TCR interaction-driven T cell responses.

8.8 Kinetics of Vav1 phosphorylation in Q59GDR4-stimulated T cells was distinct from that in M12DR4-stimulated T cells

Vav1 is a GTP/GDP exchange factor for members of the Rho-family GTPase(s) and the TCR-mediated tyrosine phosphoylation of Vav1 is important for it's function in T cells (61). Studies on Vav1-deficient T cells suggested that Vav1 is also involved in the ERK activation (70). We therefore investigated the effect of TCR ligand avidity on Vav1 phosphorylation. Although Vav1 phosphorylation was induced by the

stimulation with M12DR4 and other stimuli, the levels of phosphorylation induced by the stimulation with variant ligands (Q59GDR4 and Y61VDR4) were lower than that of M12DR4 (Fig. 15A). Moreover, TCR engagement with M12DR4 caused rapid and maximal level of Vav1 phosphorylation at 5 min after stimulation and the phospho-Vav1 accumulation returned to basal levels after 120 min. On the other hand, the weak phosphorylation of Vav1 was detected at 5 min after Q59GDR4 stimulation. Its phosphorylation reached a peak level at 30-60 min and decreased to basal level at 120 min (Fig 15B and C). These results suggested that M12DR4 and Q59GDR4 have distinct capacities to regulate the Vav1 activity. Furthermore, the kinetic pattern of Vav1 phosphorylation paralleled with that of B-Raf/ERK activation, thus suggesting a meaningful linkage between Vav1 and B-Raf/ERK activations.

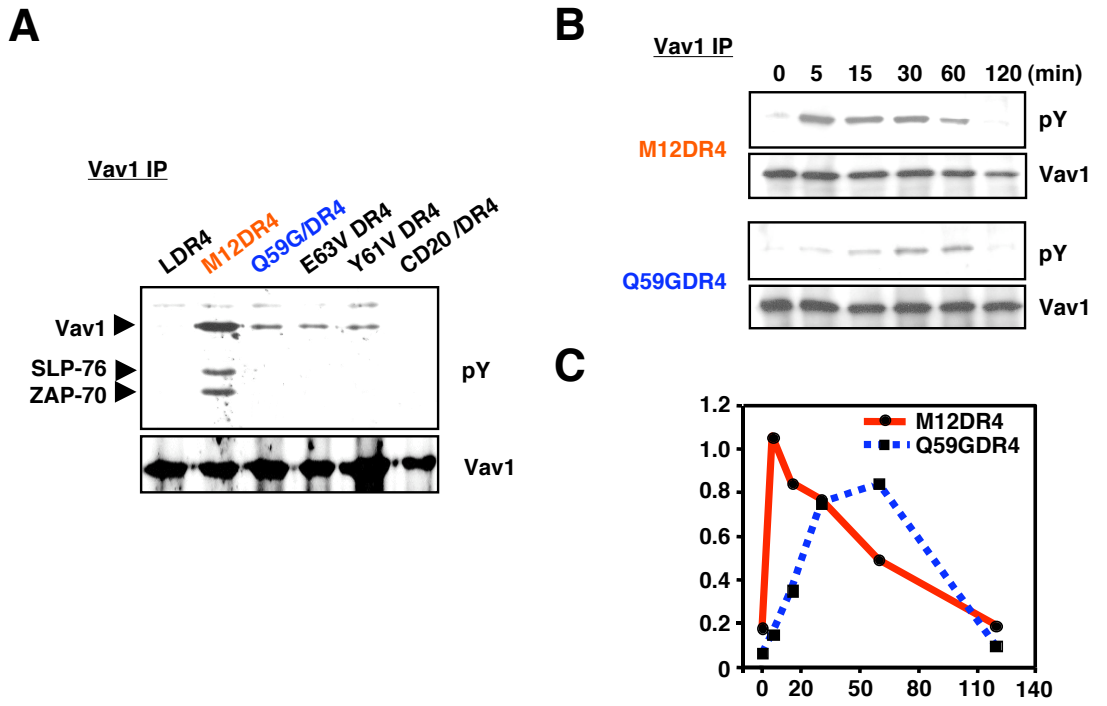

Fig. 15 The differential kinetics of Vav1 phosphorylation between M12DR4- and Q59GDR4-stimulated T cells.

A, T5-32 was stimulated with M12DR4 and its variants for 15 min. Immunoprecipitates (IP) with anti-Vav antibody from T cells stimulated in each condition were analyzed by immunoblotting with anti-phosphotyrosine (pY) (upper panel) or anti-Vav antibodies (lower panel). B. T5-32 was stimulated with M12DR4 (upper) or Q59GDR4 (#5) (lower) for indicated times. Phospho-Vav1 was shown in each

upper panel. Blotting for Vav1 confirmed the comparable loading of immunoprecipitates in each lane. Similar results were obtained in two additional experiments. C, The plot showed the ratio of phospho-Vav1/total Vav1 induced by the M12DR4 (circle) or Q59GDR4 (#5) (square) stimulation, and normalization was performed as in Fig. 3B. Values are means ± SD of triplicate experiments. Each kinetic pattern of Vav1 phosphorylation was shown as a solid line (M12DR4) and a dashed line (Q59GDR4). IP: immunoprecipitation

To study the more intensive role(s) of B-Raf in TCR-mediated T cell activation, we employed the Jurkat cells as a model system. The ease to transfect with the appropriate gene into T cells in this system allowed us to examine the molecular mechanisms of B-Raf-mediated effects in T cell activation.

8.9 TCR ligation induces both Raf-1 and B-Raf activation

Cross-linking of TCRs with soluble anti-CD3 antibody, which mimics the engagement of TCR with the agonistic peptide/MHC complex, induced ERK and MEK phosphorylation within 1 min, reaching a maximal level at approximately 1-3 min in Jurkat cells (Fig. 16A). The ERK/MEK phosphorylation displayed similar kinetics and were prolonged for up to 60 min. Next, we performed in vitro kinase assays for Raf-1 and B-Raf to estimate the strength and kinetics of their kinase activities. Consistent with the previous report (47), Raf-1 was activated at 3 min after TCR ligation, and became inactive within 20 min (Fig. 16B). In contrast to the kinetics of Raf-1 activity, there was slight but detectable B-Raf activity even under the basal condition, and B-Raf showed a pronounced increase of its kinase activity at 3 min after TCR stimulation. B-Raf kinase activity was gradually decreased, but did last for up to 60 min (Fig. 16B). Raf-1 was inactivated after 20 min of TCR ligation, nevertheless apparent MEK/ERK activation was still sustained up to 60min (Fig. 16A). Intriguingly, the kinetics of TCR-mediated B-Raf activation rather than that of Raf-1 activation was similar to that of MEK/ERK activation. Addition of co-stimulation with an anti-CD28 antibody treatment slightly enhanced the B-Raf activity over time compared with that stimulated with an anti-CD3 antibody alone (Fig. 16C).

Physiological association between Raf family kinases and MEK is necessary for MEK/ERK activation (71), hence we asked if B-Raf can interact with MEK in T cells in response to TCR stimulation using co-immunoprecipitation methods. For this purpose,

wild-type B-Raf tagged with HA was expressed in Jurkat cells and was immunoprecipitated with an anti-HA antibody. The specific association between HA-B-Raf and MEK was achieved at a maximal level at 3 min after TCR ligation and this interaction lasted for up to 60 min with a slight decrease (Fig. 16D). The intrinsic interaction between B-Raf and MEK was also evaluated by reciprocal immunoprecipitation experiments using an anti-MEK antibody to detect endogenous B-Raf protein. As shown in Fig. 2E, endogenous B-Raf protein was not detected in immunoprecipitates with the anti-MEK antibody in unstimulated Jurkat cells. Consistent with Fig. 16D, intrinsic B-Raf/MEK complex formation was strongly induced at 3 min after TCR ligation and then it decreased gradually but remained above the basal level up to 60 min after TCR stimulation in vivo (Fig. 16E). The kinetics of B-Raf/MEK interaction paralleled those of B-Raf activation (Fig. 16B). These results strongly suggested that B-Raf was involved in MEK/ERK activation stimulated with TCR ligation, especially in the late phase after Raf-1 had become inactive (Fig. 16B).

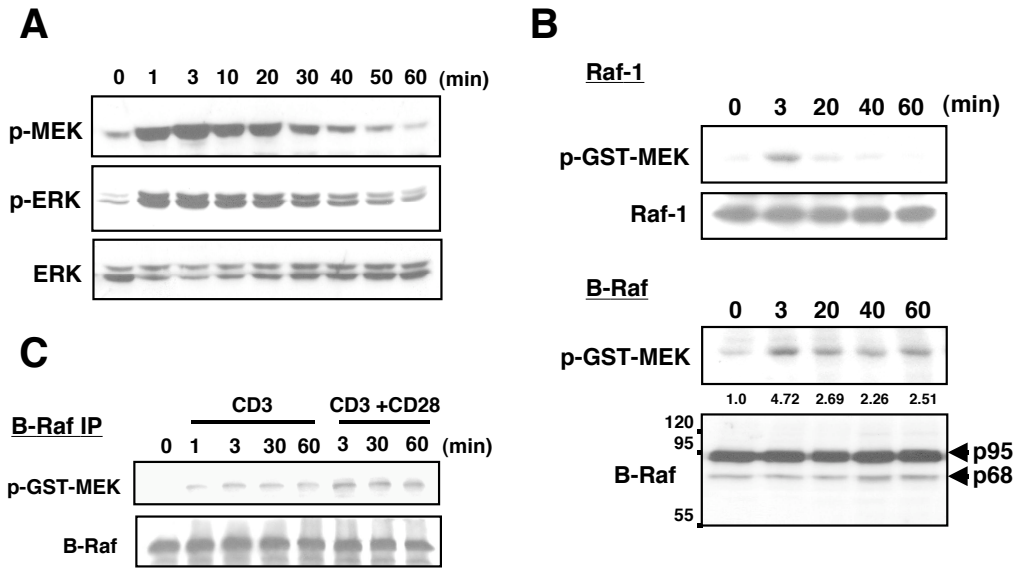

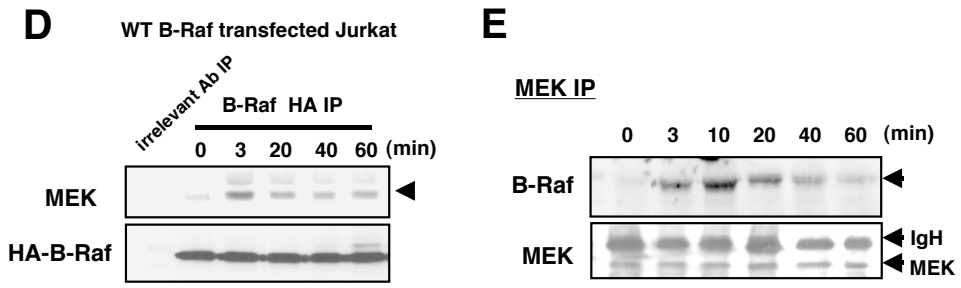

Fig. 16 B-Raf activation and B-Raf/MEK interaction were induced in a TCR stimulation-dependent manner.

A, Jurkat T cells were incubated with or without (0 min) a soluble anti-CD3 antibody together with a second antibody for the indicated time. The cells were subjected to Western blotting with an anti-phospho-MEK specific antibody (upper panel) or an anti-phospho-ERK specific antibody (middle panel). Equal protein loading was confirmed by total ERK blotting (bottom panel). B, In vitro kinase assays for Raf-1 and B-Raf isolated from Jurkat cells stimulated with the anti-CD3 antibody for the indicated time. Recombinant GST-MEK was used as a substrate and incorporated ^{32}P radioactivities were visualized by autoradiography. Equal loading of each Raf protein was confirmed by blotting with either an anti-Raf-1 antibody (upper bottom panel) or an anti-B-Raf antibody (lower bottom panel). C, Additive anti-CD28 antibody stimulation enhanced the B-Raf kinase activity. Jurkat cells were stimulated with the anti-CD3 antibody alone or the anti-CD3 together with the anti-CD28 antibodies for the indicated time and in vitro kinase assay was performed. D, TAg-Jurkat cells transiently expressing HA-tagged wild-type B-Raf were stimulated with cross-linking of soluble anti-CD3 antibody for the indicated time. Immunoprecipitates with an anti-HA antibody were blotted with an anti-MEK (upper panel) or the anti-HA antibodies (lower panel). The immunoprecipitates with irrelevant rabbit IgG in Jurkat cells stimulated for 3 min was used as a negative control. E, Immunoprecipitates with an anti-MEK antibody from Jurkat cells stimulated with the anti-CD3 antibody for the indicated time were blotted with the anti-B-Raf antibody (upper panel). The same membrane was reprobed with the anti-MEK antibody (lower panel) to monitor equal protein loading. The data are representative of three reproducible experiments in all analyses. Ab: antibody. IP: immunoprecipitation.

8.10 TCR-mediated B-Raf activation is partly dependent of Ras activity

Previous studies reported that B-Raf activation in fibroblasts was dependent on Ras activation (72,67). In other cases, Ras activity was not essential for B-Raf activation in PC12 cells (23, 38). In T cells, to determine whether Ras activity is required for the B-Raf activation, TCR-mediated B-Raf activity was measured in TAg-Jurkat expressing the dominant negative Ras mutant RasN17. The RasN17 interfered with endogenous Ras, Raf-1 and MEK/ERK activation until at least 60 min after TCR stimulation (Fig. 17A) (22). As shown in Fig. 17B, TCR engagement resulted in a robust activation of B-Raf after stimulation in mock-transfected Jurkat cells. In

contrast, RasN17-transfected cells showed decreased B-Raf activation as compared with that observed in the control cells at 3 min after TCR stimulation (75% reduction). Similar inhibitory effects was observed at any given time points. These results indicated that TCR-mediated B-Raf activation is, at least in part, regulated by Ras activation in vivo.

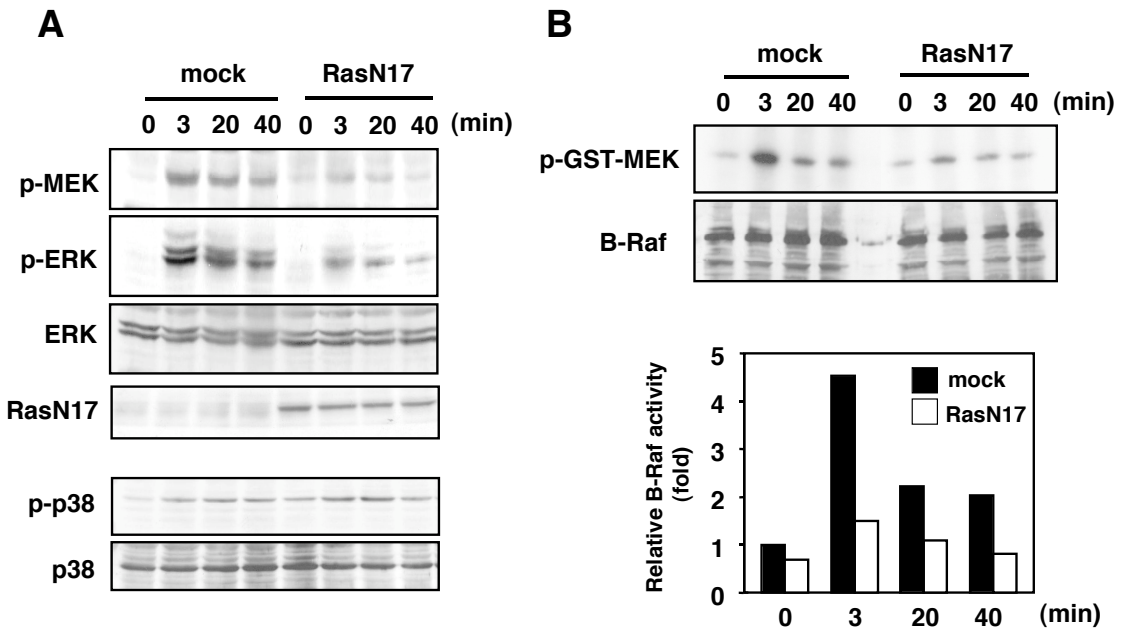

Fig. 17 Ras regulated B-Raf activation following TCR stimulation in Jurkat cells.

A, TAg-Jurkat cells were transfected with a mock vector or with the RasN17 expression vector, then, these cells were harvested and stimulated with cross-linking of soluble anti-CD3 antibody for the indicated time. Blotting with anti-p-MEK, p-ERK, ERK, T7, p-p38 and p38 are performed. B, TAg-Jurkat cells were transfected with a mock vector or with the RasN17 expression vector, then, these cells were harvested and stimulated with cross-linking of soluble anti-CD3 antibody for the indicated time. Immunoprecipitates from each cell extract with an anti-B-Raf antibody were mixed with the recombinant GST-MEK as a substrate and in vitro kinase reaction for B-Raf were performed. v Whole cell lysates (WCL) were blotted with anti-H-Ras antibody to monitor the expression of RasN17 (lower panel). The intensity of the GST-MEK phosphorylation by B-Raf immunoprecipitated from mock-transfected (black bar) or RasN17-transfected cells (white bar) was quantified by densitometric analysis. The relative B-Raf activity at 0 min in mock-transfected cells was assigned to be 1.0. Essentially similar results were obtained in three independent experiments. IP: immunoprecipitation.

8.11 B-Raf contributes to sustained MEK/ERK activation

Within the activation segment of B-Raf, there are two sites, threonine 598 (Thr 598) and serine 601 (Ser 601) which can be phosphorylated in response to Ras

activation, and phosphorylation status of these residues is required for the maximal kinase activity of B-Raf (Fig. 6 and Ref. 51 and 72). Hence, we introduced a dominant negative mutant of B-Raf (B-Raf AA), in which Thr 598 and Ser 601 were substituted to Ala (51), into T cells to examine the role of B-Raf in TCR-mediated MEK/ERK activation cascade. As shown in Fig. 18A, Jurkat clone expressing B-Raf AA showed a similar degree of MEK/ERK activation induced by TCR cross-linking with soluble anti-CD3 antibody at 3 min after stimulation in comparison to that of mock transfected cells. The MEK/ERK activation was effectively sustained for 60 min in the mock transfectants. On the other hand, in the Jurkat clone expressing B-Raf AA, MEK/ERK activation returned to the basal level within 30 min after TCR stimulation and then it was no longer detected. Densitometric analyses of MEK/ERK activation revealed that the activation kinetic pattern rather than the relative magnitude of MEK/ERK activation was distinct between the mock-transfected clone and the B-Raf AA expressing clone (Fig. 18B). Since TAg-Jurkat cells transiently transfected with B-Raf AA showed essentially similar response, the possibility that these results were specific for one particular clone (AA2) was excluded (Fig. 18C). Moreover, these results were not due to the inhibition of Raf-1 activity by B-Raf AA, because the degree of TCR-mediated Raf-1 activation in B-Raf AA expressing Jurkat cells was indistinguishable from that of mock-transfected Jurkat cells or cells expressing HA-tagged wild-type B-Raf (Fig. 18D and data not shown). In contrast to MEK/ERK activation, no significant differences in phosphorylation of other mitogen-activated protein kinase (MAPK), p38 were detectable in both mock- and B-Raf AA- transfected TAg-Jurkat cells, suggesting that B-Raf AA did not influence p38 activation (Fig. 18C). The data indicated that B-Raf physiologically and specifically regulated prolonged MEK/ERK activation induced by TCR stimulation in Jurkat cells.

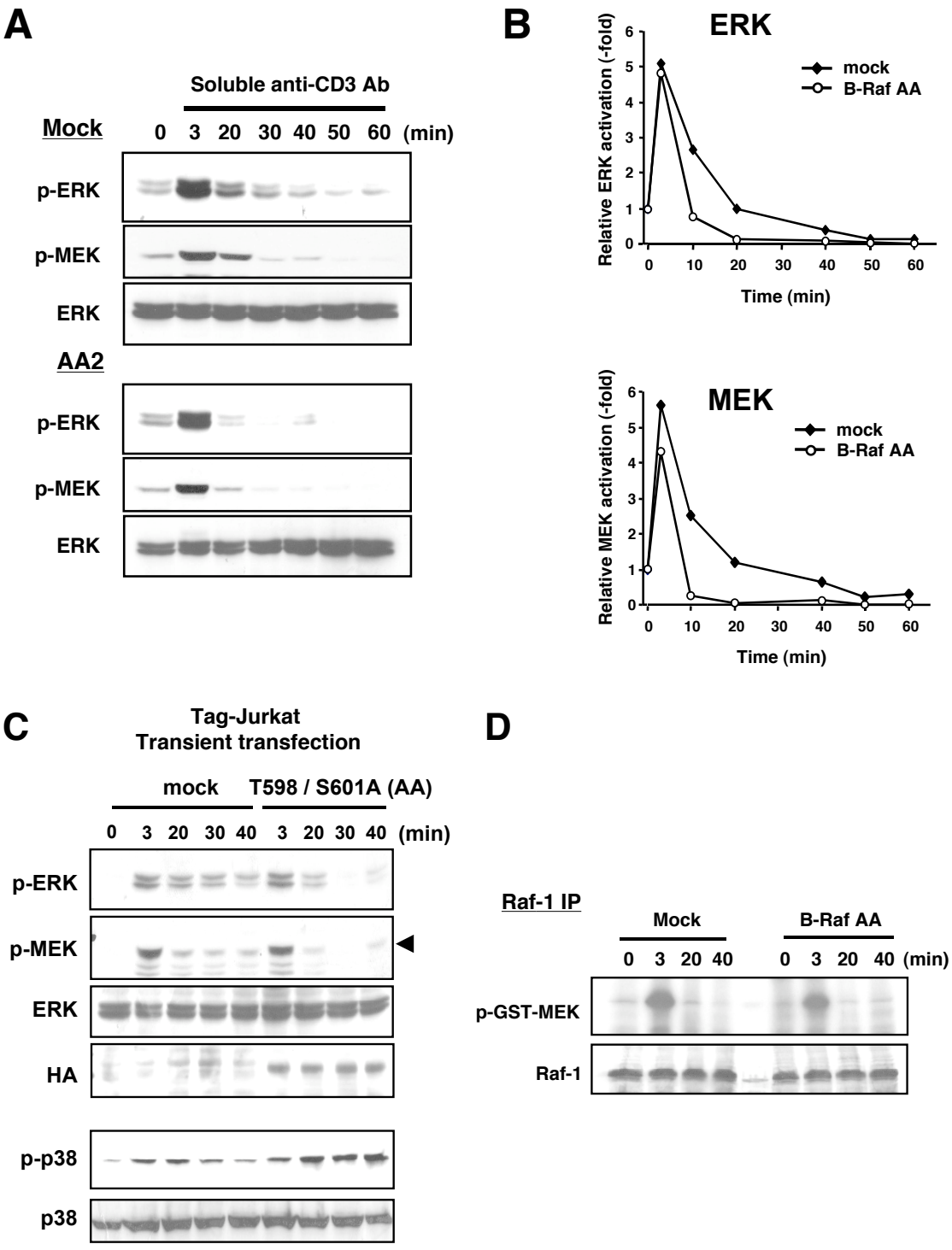
A
Soluble anti-CD3 Ab
Mock
0 3 20 30 40 50 60 (min)
p-ERK
p-MEK
ERK
AA2
p-ERK
p-MEK
ERK
B
ERK
mock
B-Raf AA
Relative ERK activation (-fold)
Time (min)
MEK
mock
B-Raf AA
Relative MEK activation (-fold)
Time (min)
C
Tag-Jurkat
Transient transfection
mock
T598 / S601A (AA)
0 3 20 30 40 3 20 30 40 (min)
p-ERK
p-MEK
ERK
HA
p-p38
p38
D
Raf-1 IP
Mock
B-Raf AA
0 3 20 40 0 3 20 40 (min)
p-GST-MEK
Raf-1

Fig. 18 Dominant negative B-Raf AA prevented T cells from inducing sustained MEK/ERK activation in response to TCR ligation.

A, Phosphorylation kinetics of MEK and ERK in Jurkat clones expressing wild-type B-Raf or B-Raf AA (AA2) induced by TCR cross-linking with soluble anti-CD3 antidbody. B, Kinetics of relative amount of phosphorylated ERK (a) and MEK (b). The relative value of intensity of phospho-protein bands divided by that of whole ERK bands at each time point observed in mock- or B-Raf AA (AA2) expressing clone were plotted. The ratio at 0 min was assigned to be 1.0. C, Western blotting analyses were done as described in A using whole cell lysates from TAg-Jurkat cells transiently transfected with mock or B-Raf AA expression vector and stimulated for the indicated time. Blottings with anti-phospho-ERK, ERK, HA (B-Raf), phospho-p38 or p38 antibodies are shown. D, TAg-Jurkat cells transiently transfected with mock vector or with B-Raf AA expression vector were stimulated with TCR cross-linking for the indicated time. In vitro kinase assays for Raf-1 were performed using immunoprecipitates from each cell extract with an anti-Raf-1 antibody (upper panel). Blotting with anti-Raf-1 antibody indicated equal protein loading (lower panel). Each result from three independent experiments was essentially the same and one is shown.

8.12 B-Raf activation and subsequently sustained ERK activation is required for full IL-2 production

As IL-2 production is one of the most critical events of ERK-mediated T cell activation, we first utilized the reporter assay controlled by IL-2 promoter element to investigate the effect of B-Raf activation on IL-2 promoter activity. Whereas TCR stimulation resulted in induction of luciferase, which reflected the IL-2 promoter activity in wild-type B-Raf transfected clone (WT30), B-Raf AA significantly attenuated the inducible IL-2 promoter activity (Fig. 19A). Indeed, as shown in Fig. 19B, TCR stimulation induced a marked increase in IL-2 production in mock-transfected Jurkat cells and in wild-type B-Raf expressing clones (WT30 and WT34), while it was substantially reduced in B-Raf AA expressing clones (AA2 and AA23).

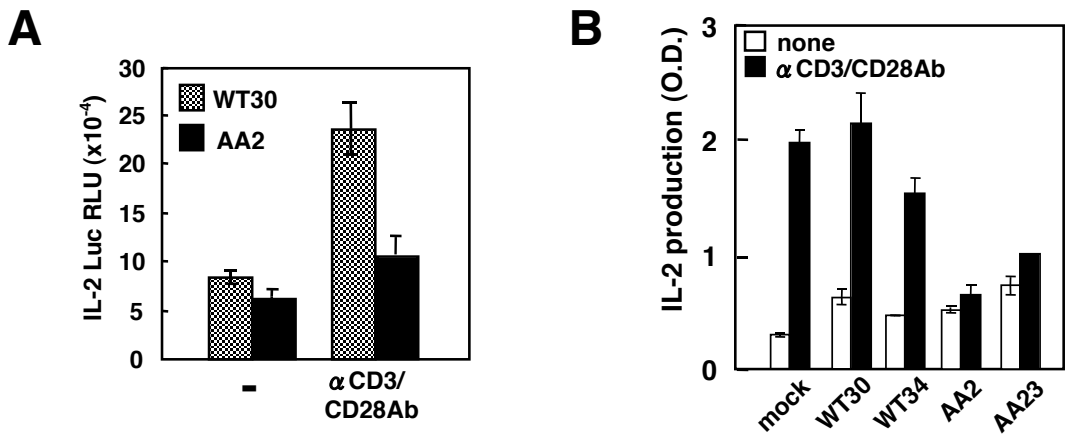

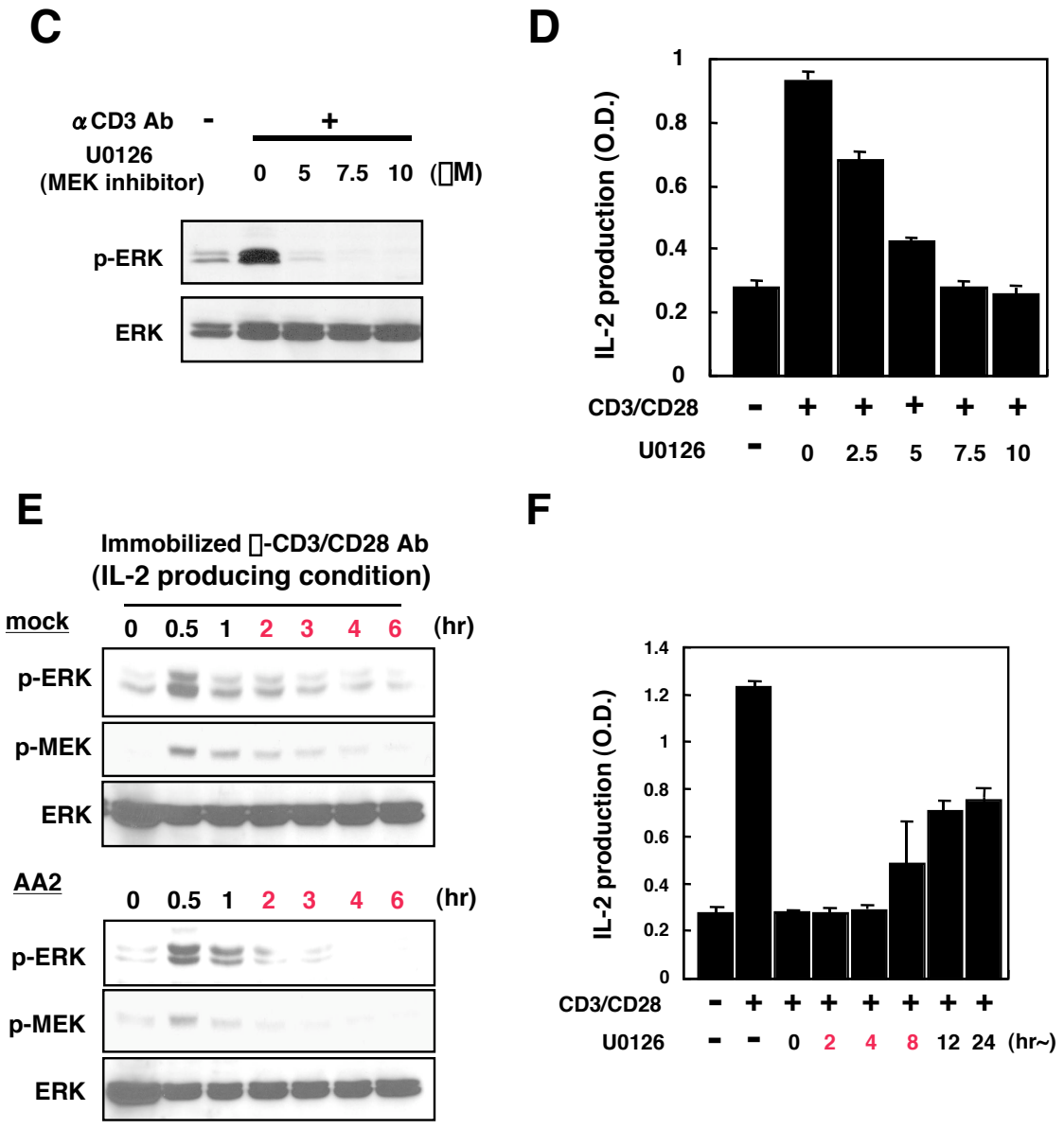

Fig. 19 Sustained ERK activation controlled by B-Raf is critical in TCR-mediated production of IL-2.

A, Luciferase assay for IL-2 promoter activity. Jurkat clone expressing wild-type B-Raf (WT30) or B-Raf AA (AA2) was transfected with an IL-2-luciferase construct and incubated with or without immobilized anti-CD3 and anti-CD28 antibodies for 12 hr. Each luciferase activity was evaluated and normalized by the co-transfected b-galactosidase activity. RLU: relative luciferase unit. B, Jurkat clones expressing wild-type B-Raf (WT30 and WT34), B-Raf AA (AA2 and AA23) and mock-transfectant were stimulated with immobilized anti-CD3 and anti-CD28 antibodies for 48 hr. IL-2 in the culture supernatants were measured by ELISA. C, Jurkat cells were pretreated with MEK inhibitor U0126 at the indicated concentrations for 30 min before stimulation, and then were stimulated with an anti-CD3 antibody for 3 min and phosphorylation of ERK was analyzed with Western blotting. D, For measurement of IL-2, as described in C, Jurkat cells pretreated with U0126 at indicated concentration were stimulated with immobilized anti-CD3 and anti-CD28 antibodies for 48 hr. IL-2 in the culture

supernatants were measured by ELISA. E, Mock transfected (upper panel) or B-Raf AA expressing Jurkat clone (AA2: lower panel) were stimulated with the immobilized anti-CD3 and anti-CD28 antibodies for the indicated time. The whole cell extract from each sample was analyzed by blotting with anti-phospho ERK (top panel), phospho MEK (middle panel) or ERK (bottom panel) antibodies, respectively. F, Vehicle (DMSO) or U0126 (5 □M) was added to the culture at the indicated times after the beginning of stimulation of Jurkat cells with immobilized anti-CD3 and anti-CD28 antibodies. After 48 hr from the start of stimulation, each culture supernatant was harvested and the IL-2 concentration was measured, as described in C. Typical data from three independent and reproducible experiments are presented here.

The data described above clearly indicated that T cells expressing B-Raf AA had defects in sustained ERK activation and subsequent full IL-2 production in comparison with the control cells in response to TCR stimulation. However, whether the sustained ERK activation is directly correlated with the full IL-2 production remained to be solved. To clarify this issue, we investigated the requirement of TCR-mediated sustained ERK activation for the IL-2 production using the pharmacological MEK inhibitor U0126. As shown in Fig. 19C, TCR-mediated ERK activation was inhibited by U0126 at the range of 5-10 □M. In addition to ERK activation, IL-2 production provoked by stimulation with immobilized anti-CD3 and CD28 antibodies was markedly blocked by U0126 at the same range of concentrations (Fig. 19D).

We also examined the effects of B-Raf AA on the magnitude and period of ERK activation stimulated with immobilized anti-CD3 and CD28 antibodies. It must be noted that, as compared with the stimulation by cross-linking of soluble anti-CD3 antibody with the second antibody (Fig. 2A), stimulation with immobilized anti-CD3 and CD28 antibodies resulted in a retardation of ERK activation and extended ERK activation in mock transfected cells (Fig. 16E). Such temporal differences in ERK activation have been reported, and the authors suggested that this phenomenon was due to the difference in TCR occupancy (73). As shown in Fig. 16E, in mock-transfected cells, TCR stimulation induced an accumulation of active ERK within 0.5 hr and this lasted for 6 hr, while the sustained ERK activation over 2 or 3 hr was impaired in cells expressing B-Raf AA. The data also confirmed that B-Raf was required for sustained ERK activation. Based on the results of Fig. 19C, 5 □M of U0126 was used to determine whether the sustained ERK activation that can be suppressed by B-Raf AA, as shown in Fig. 16D, was required for the maximal IL-2 production. Continuous

treatment of T cells with U0126 over the period of TCR stimulation abolished IL-2 production (Fig. 16F). Interestingly, addition of U0126 after 2 or 4 hr of TCR stimulation also reduced IL-2 production to a degree comparable with that of cells treated with U0126 from the beginning of stimulation although the intense ERK activation was induced for up to 2 hr after stimulation. The same condition in which B-Raf AA inhibited the sustained ERK activation can be reproduced by treatment of Jurkat cells with U0126 after 2 or 4 hr of TCR stimulation. Therefore, not only the intense ERK activation in the early phase but also the sustained ERK activation in the late phase was necessary for maximal IL-2 production. Concomitantly, these results suggested that the defect of IL-2 production in Jurkat cells expressing B-Raf AA was due to the lack of potential to maintain the TCR-mediated sustained ERK activation even though the transient ERK activation was intact.

8.13 AP-1 activation induced by TCR ligation is not impaired in Jurkat cells expressing B-Raf AA

To define more precisely the biochemical mechanisms underlying the relationship between B-Raf dependent ERK activation and IL-2 production, we first investigated the TCR-mediated c-Fos induction, one of the downstream targets of ERK (74). As shown in Fig. 6A, the expression of c-Fos was induced within 1 hr and its phosphorylation judged by electrophoretic mobility shift was potentiated by TCR stimulation in cells expressing wild-type B-Raf. There was no significant difference in c-Fos induction between Jurkat clones expressing wild-type B-Raf and B-Raf AA up to 3 hr (Fig. 20A). Next, to examine whether B-Raf contributed to AP-1 activation, we performed a luciferase assay. Consistent with c-Fos induction, the AP-1 promoter activity in response to TCR stimulation in the Jurkat clone expressing B-Raf AA (AA2) was comparable as compared with that of the control clone (WT30) (Fig. 20B). Thereby, TCR-mediated c-Fos induction and AP-1 activation seemed to be less dependent on B-Raf.

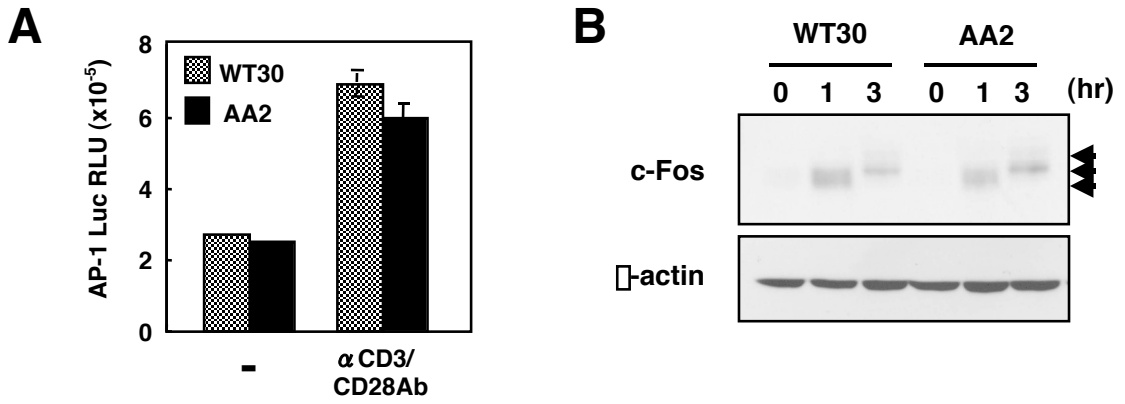

Fig. 20 B-Raf activity does not influence c-Fos induction and AP-1 activation.

A, Western blotting analysis using an anti-c-Fos antibody (upper panel). Jurkat clones expressing wild-type B-Raf (WT30) or B-Raf AA (AA2) were stimulated with immuobilized anti-CD3 antibody for the indicated time. Blotting with an anti-b-actin antibody indicated equal loading of proteins (lower panel). Arrowheads indicate the phosphorylated forms of c-Fos. B, Luciferase assay for AP-1 promoter activity. Jurkat clones expressing wild-type B-Raf (WT30) or B-Raf AA (AA2) together with an AP-1-luciferase construct were stimulated with immobilized anti-CD3 and anti-CD28 antibodies for 8 hr followed by a 12 hr culture. Each luciferase activity was measured and normalized by the co-transfected b-galactosidase activity. RLU: relative luciferase unit. The data are representative of three independent and reproducible experiments. Ab: antibody.

8.14 B-Raf activity is important for TCR-mediated NFAT activation

The IL-2 production is regulated by nuclear translocation and activation of the NFAT transcription factor cooperating with the AP-1 components c-Fos and c-Jun (27,28,29). Thus, NFAT-dependent transcriptional events in T cells require the simultaneous activation of multiple Ras effectors such as the ERK and JNK pathways (75). We analyzed whether TCR-mediated B-Raf activity would influence NFAT activation, using an NFAT-GFP reporter. In Jurkat transfected with NFAT-GFP reporter, the treatment of pharmacological agents, PMA and Ionomycin induced the GFP expression, which is regulated by a promoter corresponding to NFAT binding site. This expression was significantly blocked by a calcineurin inhibitor, cyclosporine A (Fig. 21A), suggesting that GFP expression is actually derived from NFAT promoter activity. We next performed this assay using B-Raf AA expressing Jurkat. GFP expression, which is regulated by a promoter corresponding to NFAT binding site, is increased in a TCR stimulation dependent manner in mock-transfected cells (Fig. 21B).

Comparable transfection efficiency was monitored by co-transfection of a DsRed expression vector (data not shown). In contrast, GFP expression was significantly suppressed in B-Raf AA expressing cells, suggesting that B-Raf activity is important for the regulation of TCR-mediated NFAT activity. Given that B-Raf regulated TCR-mediated MEK/ERK activation in late phase, there is a possibility that B-Raf activation couples NFAT activation to MEK/ERK activation. For confirmation, we analyzed whether the inhibition of ERK activity in the late phase blocks NFAT reporter activity. As expected, the TCR stimulation-induced GFP expression was reduced by pre-treatment with U0126 (Fig. 21C). Furthermore, similar to IL-2 production, the inhibition of NFAT reporter activity was also observed in the presence of U0126 after 2 hr of TCR stimulation, although this suppression was less effective than that observed in simultaneous U0126 treatment at the beginning of the TCR stimulation. These results suggested that not only transient but also sustained ERK activation was necessary for the TCR-mediated NFAT activation.

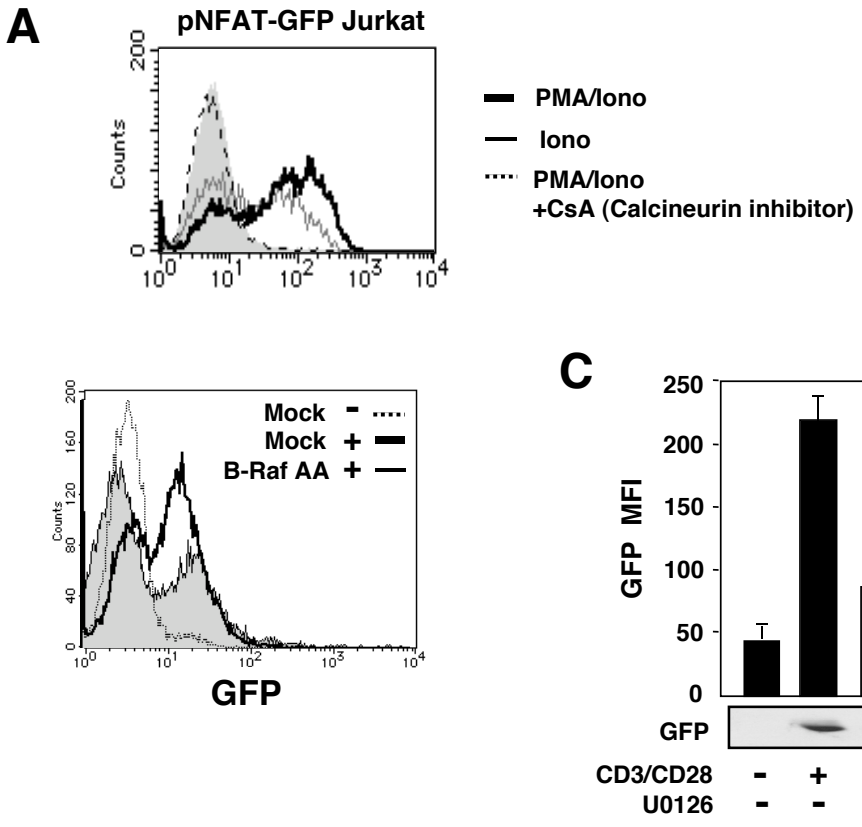

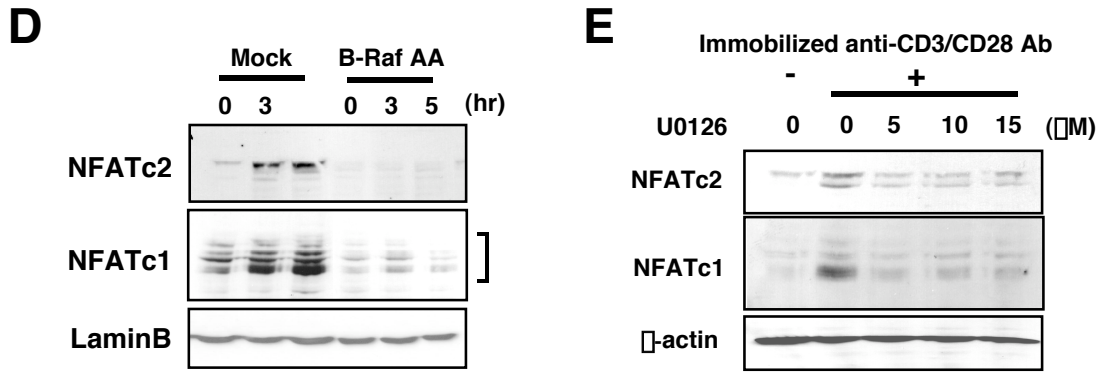

Fig. 21 B-Raf activity is required for NFAT activation.

A, Tag-Jurkat cells transfected with the NFAT-GFP reporter construct, and they were stimulated with or without PMA and Ionomycin. The treatment of cyclosporin A (CsA) was performed for 30 min before TCR stimulation. Twelve hours after stimulation, GFP expression was assessed by flow cytometric analyses. B, TAg-Jurkat cells co-transfected with the NFAT-GFP reporter construct and mock or B-Raf AA expression vector were stimulated with (+) or without (-) immobilized anti-CD3 and anti-CD28 antibodies for 9 hr. A representative flow cytometric profile for GFP expression is shown. C, NFAT-GFP transfected Jurkat cells were stimulated and then GFP expression was examined by blotting with anti-GFP antibody (lower panel) and flow cytometry (upper panel). The diagram represents the average of GFP mean fluorescence intensity (MFI) obtained from three independent experiments. U0126 (5 □M) was added to the culture at 0 hr or 2 hr after TCR stimulation. D, Nuclear extracts were isolated from mock- or B-Raf AA-transfected cells stimulated with or without immobilized anti-CD3 and anti-CD28 antibodies for indicated time. Then, the nuclear fractions were separated by SDS-PAGE and the translocation into nucleus of NFAT1 and NFAT2 were analyzed by western blotting. Blotting with anti-Lamin B antibody indicated the appropriate nuclear fractionation and protein loading. E, NFAT-GFP-transfected Jurkat cells were pretreatment with or without U0126, and stimulated with immnobilized anti-CD3 and CD28 antibodies. As described in D, the translocation into nucleus of NFAT1 and NFAT2 were analyzed by western blotting. Essentially similar results were obtained in three independent experiments.

Upon TCR stimulation, NFAT proteins are dephosphorylated by calcineurin, translocates into the nucleus, and then binds to cognate DNA elements (29). Finally, to dissect the mechanism responsible for the B-Raf mediated induction of NFAT activity, we evaluated the nuclear translocation of NFAT protein induced by TCR stimulation. As shown in Fig. 21D, the stimulation of mock-transfected Jurkat cells with TCR ligation drove the translocation of NFAT1 and NFAT2 into nucleus at 3 and 5 hr of TCR stimulation. In contrast, the substantial nuclear translocation of NFAT1 and NFAT2 could not observed in B-Raf AA expressing Jurkat cells under either non-stimulated or TCR-stimulated condition. Equal loading of nuclear protein in both cells was

estimated by blotting of Lamin B as a nuclear marker. It is most likely that defect of NFAT activity in B-Raf AA expressing cells was due to the aberrant nuclear translocation of NFAT1 and NFAT2. We hypothesized that these inhibitory effects of B-Raf AA on TCR-mediated NFAT activation were partially due to the attenuation of B-Raf-mediated ERK activity. Given the possibility of meaning linkage between NFAT and ERK activation, we analyzed whether the blockade of ERK activity influences the TCR-mediated NFAT translocation. As expected, ERK inhibitor, U0126 attenuated the NFAT translocation in a dose dependent manner (Fig. 21E). Accordingly, these results suggest that TCR-mediated NFAT activation relies on prolonged B-Raf/MEK/ERK activation and that the attenuation of NFAT activation by B-Raf AA reflects the inhibition of TCR-stimulated IL-2 production.

9. Discussion

9.1 The avidity of TCR ligand affected the TCR signal transduction

Under physiological conditions, consistent with the flexibility of the TCR-peptide/MHC interaction, various signaling events and subsequent cellular responses by TCR ligation is induced in an escalated manner rather than on/off phenomenon in a variety of ways depending on the strength and quality of the stimulus (3,14,16,73). One of the aims of our study is to clarify the effect of TCR ligand avidity on TCR-mediated signal transduction in T cell responses. Based on our results, we suggested that the differences in avidity of TCR-peptide/MHC interactions modulate the strength and duration of the B-Raf/Raf-1/ERK activation.

Q59G peptide is an analogue of M12 agonistic peptide and was originally identified as a partially agonistic APL for cognate T cell clone (8). A small number of Q59G/HLA-DR4 complexes could not fulfill the stimulatory capacity to induce the substantial T cell proliferation due to relatively weak affinity/avidity for TCR (Fig. 7A and Ref. (8)). However, as the density increased, the ligand avidity of Q59G/HLA-DR4 complexes for cognate T cells was augmented, resulting in the induction of sufficient T cell activation such as cytokine gene transcription and cell-cycle progression. Furthermore, our experimental approach allowed us to detect the augmented faint alterations of TCR signalings such as slight and delayed B-Raf/ERK activation induced by the low-avidity TCR ligand (Fig. 13), which is too faint to be detected under subtle physiological conditions in antigen specific human T cells.

It is widely accepted that some APLs, representative low-affinity/avidity TCR ligands, triggers intracellular signals that are qualitatively distinct from those stimulated with the original agonistic ligands due to their short half-life of interaction with cognate TCR (13-16). Supporting this assumption, as summarized in Fig. 22, agonistic ligand, M12/HLA-DR4 complexes induced an immediate ERK activation followed by a gradual reversion of ERK activation into their resting state. On the other hand, Q59G/HLA-DR4 complexes-evoked signals resulted in an opposite phenomenon, the delayed ERK activation. Collectively, we demonstrated that the difference of avidity influenced to TCR signaling qualitatively and quantitatively, and then increasing density of Q59G/HLA-DR4 complex on APC restored the delay of activation onset and

extended the duration of ERK activation (Fig. 13B and 22). Other study demonstrated similar phenomena in T cells stimulated with the low-affinity APL stimulation, in which the APL stimulation caused retardation in calcium influx (16) and an accumulation of phospho-c-jun in murine $CD8^+$ T cells (14).

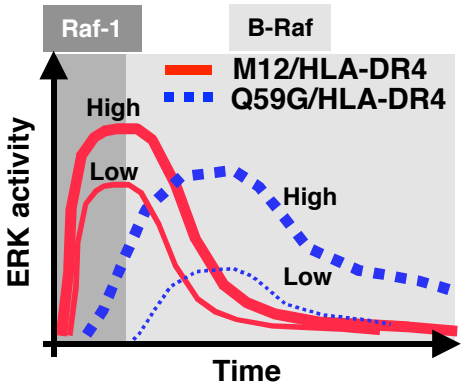

Fig. 22 A schematic model for ERK activation defined by TCR ligand avidity. The duration and strength of TCR-mediated ERK activity are determined by TCR ligand avidity. High-avidity interactions with M12/HLA-DR4 complexes at high (bold line) or low (thin line) density induce intense and immediate ERK activation mediated by Raf-1 and B-Raf, whereas the relatively low-avidity interactions with Q59G/HLA-DR4 complexes at high (bold dotted line) or low density (thin dotted lines) trigger the retarded activation mediated by B-Raf. Distinct kinetics and extent of accumulation of B-Raf/Raf-1/ERK activation may be the consequence of the dynamics of TCR engagement with differential half-life of interactions.

Our findings provide the novel insight about the intracellular signaling for the mechanism of T cell activation postulated by the kinetic proofreading hypothesis and TCR serial triggering model (17,18). In these models, the extent of accumulation of signaling events has been suggested to be influenced by the level of antigenic stimulation, which was determined by the stimulus dose as well as TCR-peptide/MHC dissociation rate (14,17,18,73). Accordingly, the differences in dissociation rate and consequently the frequency of TCR engagement can explain the differences between M12 and Q59G/HLA-DR4 complex in regard to their ability to induce B-Raf/Raf-1/ERK activation through the same TCR. Since the rate and extent of accumulation of active ERK were determined by the level of TCR engagement, the delay in ERK activation in Q59GDR4-stimulated T cells would be a consequence of the time required to exceed a threshold level by the accumulation of incremental activation signals by

simultaneous but less effective engagement of multiple TCRs. Indeed, Q59GDR4 stimulation was drastically less efficient in induction of TCR down-modulation that was an index of the productive TCR triggering than were M12DR4 stimulation (Fig. 8B). Furthermore, this might be one possible cause for the sustained B-Raf/ERK activation in Q59GDR4-stimulated T cells, since absence of TCR down-modulation led the unlimited ligation of TCR, and then continuous input of subtle signal through the TCR.

9.2 The activation mechanisms of Raf kinases in TCR-mediated signalings

Although both Raf-1 and B-Raf seem to share some functions in regulation of the MEK/ERK activation and cellular responses (56,66,67), it also has been suggested that these two Raf kinase have their unique regulatory functions for MEK/ERK activation in TCR-mediated activation (56,76). We herein demonstrated that the attenuation of B-Raf activity with dominant negative B-Raf (B-Raf AA) or B-Raf knockdown with RNAi abrogated the T cell activation in both M12DR4- and Q59GDR4-stimulated T cells. This inhibitory effect of B-Raf AA on Q59GDR4-stimulated T cells was more prominent than that in M12DR4-stimulated T cells. This is likely due to the lack of any apparent activation of Raf-1 in Q59GDR4-stimulated T cells and therefore, only B-Raf is responsible for the MEK/ERK activation. On the other hand, the suppressive effect of B-Raf AA on M12DR4-stimulated T cell activation was modest, thus suggesting some functional redundancy between B-Raf and Raf-1, because both Raf-1 and B-Raf were activated in this condition. However, M12DR4-induced Raf-1 activation did not completely compensate the inhibition of B-Raf activation, implying the specific role(s) of B-Raf on TCR-mediated activation. Taken together, combined with the results that low-density of Q59G/HLA-DR4 molecule could not lead the substantial B-Raf/ERK activation and subsequent T cell responses, the principal experimental findings in this study make it possible to conclude that the sustained accumulation of B-Raf/ERK activation events lasting for a certain time is indispensable for the T cell responses stimulated with low-avidity TCR interactions.

The activities of both Raf-1 and B-Raf depend on Ras activation (51,56,66,67). In addition, the tyrosine phosphorylation at Tyr 340/341 by Src kinase is also required for the Raf-1 activity, whereas B-Raf lacks corresponding Tyr residues, and is therefore

less dependent on Src kinases (66,67). In T cells, it was reported that the activation of Src kinase, lck is required for the TCR-mediated Raf-1 activation (65). However, it was demonstrated that APL stimulation could not induce intense Lck activation (13). Thus, the inability to induce Raf-1 activation by Q59G/DR4 might be due to an insufficient activation of Lck. Therefore, it is conceivable that B-Raf has a lower activation threshold than Raf-1 does, and Q59GDR4 stimulation could preferentially activate B-Raf rather than Raf-1. In addition, conserved B-Raf Ser 445 corresponding to Ser 338 in Raf-1, which is one of the regulatory phosphorylation sites of Raf activity is constitutively phosphorylated in fibroblasts (66). The selective loss of activation such as Raf-1 activation in Q59GDR4 stimulated T cells imply the presence of a hierarchy in TCR-mediated signalings that is sensitive to the affinity/avidity of TCR-peptide/MHC interaction. Furthermore, these results seem to explain the fact that B-Raf exhibits a higher intrinsic kinase activity in a quiescent situation, and once stimulated, lower activation threshold and longer activation period than does Raf-1 in our and other systems.

Rap1 activity also has been postulated to suppress Ras/Raf-1/ERK cascade in vitro (62). However, in transgenic T cells that express the constitutively active form of Rap1, TCR-mediated ERK activation and CD69 up-regulation is normal, rather not impaired (77). On the other hand, Rap1 is though to be a positive regulator of B-Raf (68) and recent study showed that forced expression of B-Raf in T cells enhanced the ERK activation and CD69 up-regulation (78). Thus, it is possible that Rap can act as an activator of Ras/B-Raf/ERK cascade through B-Raf activation in some conditions. In this study, we demonstrated that not only M12DR4 stimulation but also Q59GDR4 stimulation provoked the Rap1 activation in comparable degree. Although these findings may support the hypothesis that Rap1 activation is also prerequisite for B-Raf activation in T cells, the details of the molecular mechanisms how Rap1, in addition to Ras regulate the B-Raf activation should be further investigated.

In addition to Rap1, Ras activation is indispensable for maximal B-Raf activation (56,66,67), and its activation was also induced in Q59GDR4-stimulated T cells as well as in M12DR4-stimulated T cells. However, it is unlikely that Ras and Rap1 activation is actually enough to activate the B-Raf because the activation kinetics did

not coincide with those of B-Raf activation in Q59GDR4-stimulated T cells. These results suggest that TCR-mediated Ras and Rap1 activation is not sufficient for B-Raf/ERK activation and the additional modifier(s) of B-Raf/ERK cooperating with Ras and Rap1 exists in an up-stream of B-Raf. The most straightforward explanation for the delay in B-Raf/ERK activation might be that it reflects the time required for the accumulation of active modifier(s) to reach the threshold level for induction of their activations. In both M12DR4- and Q59GDR4-stimulated T cells, the kinetic changes of Vav1 phosphorylation were quite similar to those of B-Raf/ERK activation (Fig. 15), suggesting Vav1 as a B-Raf/ERK modifier. In accordance with this interpretation, the following findings are reported: 1) Although Vav1 can act as a Rac-specific GEF in vitro, an over-expression of Vav1 in Jurkat T cells augmented the TCR-mediated ERK activation and CD69 up-regulation. This effect was due to the synergy of Vav1 with Ras activations and it was independent of the GEF activity for Rac of Vav1 (79,80). 2) low-avidity APL stimulation has been shown to induce a weak phosphorylation of Vav1 (Fig. 15 and Ref.13). 3) It was recently demonstrated that in Vav1 deficient $CD4^+CD8^+$ double positive thymocytes, B-Raf failed to be activated with TCR stimulation, resulting in an impaired ERK activation (76). Thus, in addition to these supportive evidences, we can propose the possibility that Vav1 is a likely modifier of the B-Raf activity that causes an altered ERK activation in T cells stimulated with low-avidity TCR interactions.

9.3 B-Raf in T cell activation stimulated with low-avidity TCR ligation

Our data presented herein promoted the notion that T cells can discriminate the subtle differences in interactions between TCR and structurally similar TCR ligands, which reflected the “qualitative” and “quantitative” balance of the intracellular signaling. In vivo circumstance, one of the critical roles of low-avidity interaction is facilitation of “homeostatic proliferation” to maintain the number of peripheral T cells in steady-state in periphery (6,12,81). An another representative role of low-avidity interaction with TCR are initiation and completion of positive selection in thymus (2,9). In this regard, interesting study of Mariathasan et al. demonstrated that positively selected stimulation (low-avidity interaction) induced sustained weak ERK activation, whereas negatively

selected stimulation (high-avidity interaction) induced transient intense ERK activation (34,82). It is noteworthy that these phenomena are essentially identical with our results in this study, which led us to speculate that B-Raf/ERK pathway may be involved in low-avidity TCR ligands-induced T cell responses such as thymic positive selection and homeostatic proliferation.

9.4 ERK and Raf kinase activation in TCR-mediated signaling

Although it is well studied that receptor-mediated signals activate the Raf/MEK/ERK cascade, precise mechanisms how the TCR signal provoke the cellular response through Raf/MEK/ERK activation has remained to be investigated. In this study, we found a novel ERK activation pathway through B-Raf, which is necessary for substantial T cell activation stimulated with TCR engagement, including low avidity TCR ligation. In mouse models, both Raf-1- and B-Raf-deficient mouse resulted in embryonic lethality (40,83), indicating conclusively that the function of both Raf isoforms for embryogenesis are not completely overlapping. However, it is poorly understood whether the three Raf isoforms have functional redundancy, or the Raf isoforms play specific role(s) for T cell activation. Until recently, Raf-1 has been considered to be a major signaling mediator for MEK/ERK activation in TCR-stimulated T cells (47,84). Our observations provided evidence that the functions of B-Raf for TCR-mediated activation do not entirely overlap those of other Raf proteins. We elucidated that B-Raf activation couples Ras with TCR-mediated MEK/ERK activation and is indispensable for prolongation of substantial MEK/ERK activation in vivo (Fig. 23).

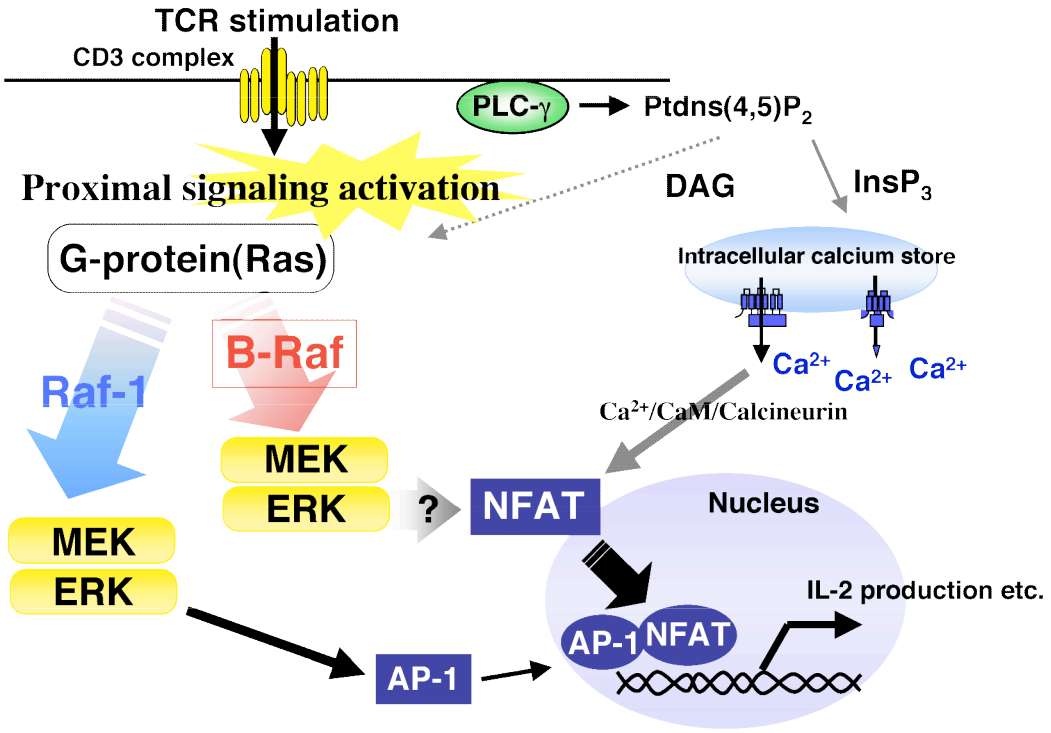

Fig. 23 TCR-mediated B-Raf activation regulates IL-2 production in human T cells.

It should be noted that the dominant negative mutant of B-Raf (B-Raf AA) did not impair the transient MEK/ERK activation but did suppress the sustained MEK/ERK activation although B-Raf was activated and associated with MEK in both the early and the late phase after TCR stimulation. Why was not MEK/ERK activation in the early phase drastically attenuated by B-Raf AA? A most likely explanation is that Raf-1 can compensate for the defects of B-Raf activation due to the functional redundancy between Raf-1 and B-Raf in early phase. The idea was supported by our observations: the B-Raf AA did not grossly perturb ERK activation when Raf -1 was active in 3-20 min after TCR stimulation (Figs. 16 and 18), suggesting that Raf-1 activity is sufficient to induce ERK activation in the early phase. On the other hand, ERK activation in the late phase (20 min □) was abrogated by B-Raf AA because the kinase activity of Raf-1 declined and Raf-1 could no longer compensate for B-Raf activity. Consequently, although we could not exclude the possibility that Raf-1 activity in early phase modulates the TCR-mediated B-Raf activation, our observations lead to the model that

Raf-1 activity is responsible and sufficient for the early phase MEK/ERK activation while B-Raf activity is essential for the late phase MEK/ERK activation in TCR-stimulated T cells.

ERK activation is critical for the precise outcome of T cell activation, including IL-2 production (27,35). The marked decrease in IL-2 production in T cells by the expression of B-Raf AA and by the inhibition of the late phase ERK activation using U0126 leads to the conclusion that ERK activation in the late phase regulated by B-Raf was critical for the full IL-2 production in response to TCR stimulation. In view of no defect of TCR-mediated c-Fos induction and AP-1 activation in Jurkat cells expressing B-Raf AA, it was indicated that these events were less dependent on B-Raf activity. In contrast to AP-1 activation, we found that B-Raf AA inhibited TCR-mediated nuclear translocation of NFAT and NFAT-mediated reporter activation (Figs. 20, 21, 23). The correlation between B-Raf and these transcriptional factors was also noted by Brummer *et al*. (44), who reported that in B-Raf null chicken B cells, B cell receptor-mediated ERK activation was eliminated in only late phase, while c-Fos induction was not abrogated. On the contrary, the loss of B-Raf expression resulted in significant defects in the B cell receptor-mediated activation of NFAT transcription factor, suggesting that NFAT activation is regulated by B-Raf in chicken B cells. The selective role of TCR-mediated B-Raf activation in NFAT regulation was consistent with that observed in B cells and their regulatory mechanisms may be conserved between immunoreceptor-mediated activation in both B and T cells. These results suggest that NFAT-responsible transcriptions and subsequent IL-2 production were dependent on B-Raf, and that Raf-1 induced ERK activation in the early phase is not sufficient to provoke these immunoreceptor-mediated activations.

It was expected that the inhibitory effect of B-Raf AA on NFAT activation was due to a defect in sustained ERK activation mediated by B-Raf because the treatment of Jurkat cells with MEK inhibitor also reduced the NFAT activation. Evidence has been accumulated that support the contribution of ERK signaling to NFAT activation. Transcriptional activity of NFAT was reported to be regulated by Ras/MEK/ERK signals acting in synergy with calcium/calmodulin phosphatase, calcineurin signals in T cells (27,75). Moreover, the mechanism by which some kinases and phosphatases

regulate the NFAT activity imply modulation of nuclear translocation of this factor, its binding to DNA or transactivation of its target gene expression. Because B-Raf AA abrogated the nuclear localization and transcriptional activity of NFAT, we propose the model that sustained B-Raf/MEK/ERK activation modulating NFAT-dependent transcription could be achieved by regulation of intrinsic nuclear translocation of NFAT. Supporting this interpretation, it has been reported that ERK1 overexpression augmented the DNA binding activity of NFAT, resulting in NFAT activation in Jurkat cells (85). However, it has been implicated that activated ERK binds to and phosphorylates NFAT2, which negatively regulates nuclear translocation and activation of NFAT2 in fibroblasts (86). Reversely, in Jurkat cells, we observed the attenuation of TCR-stimulated nuclear translocation of NFAT by MEK inhibitor (Fig. 21). These seemingly discrepant results might be accounted for by use of different systems and cell types. In any cases, the formal demonstration of a role for B-Raf and ERK in the regulation of NFAT activation in vivo requires more detailed analysis.

9.5 The significance of temporal regulation of B-Raf/ERK activation

It is noteworthy that temporal difference in the Raf-induced ERK activation signal induces qualitatively different cellular responses. In PC12 cells, EGF-driven proliferation was coupled with transient ERK activation. On the contrary, NGF-driven differentiation of PC12 cells into sympathetic neurons was induced by sustained ERK activation (30), which was mediated by B-Raf (43). A similar phenomenon was found in T cells. Mariathasan *et al.* demonstrated that in thymocytes, negatively selecting stimuli by agonistic peptides through TCR induced transient and strong ERK activation, resulting in cell death while positively selecting stimuli by the analogue peptides induced sustained and weak ERK activation, resulting in cell survival (82). In a very recent study, it has been reported that B-Raf but not Raf-1 was activated with TCR stimulation in $CD4^+CD8^+$ double positive thymocytes (76). These observations and our findings that B-Raf and Raf-1 activities regulated the strength and the duration of TCR-mediated ERK activation prompted us to consider that the Ras/B-Raf/MEK/ERK pathway also could play important roles in determining the cell fate such as thymocytes differentiation regulated by temporally distinct ERK activity.

10. Conclusions

Based on our study about TCR signaling provoked by low avidity TCR ligand, we herein suggested that 1) difference of avidity influence to TCR signaling qualitatively and quantitatively, 2) both Raf-1 and B-Raf contribute to TCR-mediated ERK activation, 3) TCR-mediated B-Raf activation is more sensitive to low avidity TCR interaction. Regarding the molecular mechanisms in B-Raf-mediated signal transduction, our data suggest that Ras/B-Raf/MEK/ERK can serve as a novel component of signaling pathways that regulate the duration of ERK activity in response to TCR stimulation. We provide the evidences that B-Raf activation is responsible for substantial T cell activation through sustained ERK and NFAT activation. We suggested that B-Raf and ERK activation with a proper duration determines the biological outcomes such as IL-2 production in human T cells. More intensive analyses of T cell activation stimulated with low-avidity TCR ligands would provide us a new biochemical profile of T cell activation that plays relevant roles in the regulation of the appropriate T-cell immune response.

11. References

1. Hogquist, K. A., Starr, T. K., and Jameson, S. C. (2003) *Curr Biol* **13**, R239-241
2. Starr, T. K., Jameson, S. C., and Hogquist, K. A. (2003) *Annu Rev Immunol* **21**, 139-176
3. Germain, R. N., and Stefanova, I. (1999) *Annu Rev Immunol* **17**, 467-522
4. Brocker, T. (1997) *J Exp Med* **186**, 1223-1232
5. Matsushita, S., Kohsaka, H., and Nishimura, Y. (1997) *J Immunol* **158**, 5685-5691
6. Kassiotis, G., Zamoyska, R., and Stockinger, B. (2003) *J Exp Med* **197**, 1007-1016
7. Stefanova, I., Dorfman, J. R., and Germain, R. N. (2002) *Nature* **420**, 429-434
8. Chen, Y. Z., Matsushita, S., and Nishimura, Y. (1996) *J Immunol* **157**, 3783-3790
9. Hogquist, K. A., Jameson, S. C., Heath, W. R., Howard, J. L., Bevan, M. J., and Carbone, F. R. (1994) *Cell* **76**, 17-27
10. Karin, N., Mitchell, D. J., Brocke, S., Ling, N., and Steinman, L. (1994) *J Exp Med* **180**, 2227-2237
11. Young, D. A., Lowe, L. D., Booth, S. S., Whitters, M. J., Nicholson, L., Kuchroo, V. K., and Collins, M. (2000) *J Immunol* **164**, 3563-3572
12. Goldrath, A. W., and Bevan, M. J. (1999) *Immunity* **11**, 183-190
13. Huang, J., Tilly, D., Altman, A., Sugie, K., and Grey, H. M. (2000) *Proc Natl Acad Sci U S A* **97**, 10923-10929
14. Rosette, C., Werlen, G., Daniels, M. A., Holman, P. O., Alam, S. M., Travers, P. J., Gascoigne, N. R., Palmer, E., and Jameson, S. C. (2001) *Immunity* **15**, 59-70
15. Irie, A., Chen, Y. Z., Tsukamoto, H., Jotsuka, T., Masuda, M., and Nishimura, Y. (2003) *Eur J Immunol* **33**, 1497-1507
16. Wulfing, C., Rabinowitz, J. D., Beeson, C., Sjaastad, M. D., McConnell, H. M., and Davis, M. M. (1997) *J Exp Med* **185**, 1815-1825
17. Rachmilewitz, J., and Lanzavecchia, A. (2002) *Trends Immunol* **23**, 592-595
18. Rabinowitz, J. D., Beeson, C., Lyons, D. S., Davis, M. M., and McConnell, H. M. (1996) *Proc Natl Acad Sci U S A* **93**, 1401-1405

19. Fremont, D. H., Hendrickson, W. A., Marrack, P., and Kappler, J. (1996) *Science* **272**, 1001-1004
20. Delon, J., Bercovici, N., Raposo, G., Liblau, R., and Trautmann, A. (1998) *J Exp Med* **188**, 1473-1484
21. Wulfing, C., Sumen, C., Sjaastad, M. D., Wu, L. C., Dustin, M. L., and Davis, M. M. (2002) *Nat Immunol* **3**, 42-47
22. Genot, E., and Cantrell, D. A. (2000) *Curr Opin Immunol* **12**, 289-294
23. D'Ambrosio, D., Cantrell, D. A., Frati, L., Santoni, A., and Testi, R. (1994) *Eur J Immunol* **24**, 616-620
24. Carey, K. D., Dillon, T. J., Schmitt, J. M., Baird, A. M., Holdorf, A. D., Straus, D. B., Shaw, A. S., and Stork, P. J. (2000) *Mol Cell Biol* **20**, 8409-8419
25. Katagiri, K., Hattori, M., Minato, N., and Kinashi, T. (2002) *Mol Cell Biol* **22**, 1001-1015
26. Rincon, M. (2001) *Curr Opin Immunol* **13**, 339-345
27. Whitehurst, C. E., and Geppert, T. D. (1996) *J Immunol* **156**, 1020-1029
28. Faris, M., Kokot, N., Lee, L., and Nel, A. E. (1996) *J Biol Chem* **271**, 27366-27373
29. Hogan, P. G., Chen, L., Nardone, J., and Rao, A. (2003) *Genes Dev* **17**, 2205-2232
30. Marshall, C. J. (1995) *Cell* **80**, 179-185
31. Bommhardt, U., Scheuring, Y., Bickel, C., Zamoyska, R., and Hunig, T. (2000) *J Immunol* **164**, 2326-2337
32. van den Brink, M. R., Kapeller, R., Pratt, J. C., Chang, J. H., and Burakoff, S. J. (1999) *J Biol Chem* **274**, 11178-11185
33. Pages, G., Guerin, S., Grall, D., Bonino, F., Smith, A., Anjuere, F., Auberger, P., and Pouyssegur, J. (1999) *Science* **286**, 1374-1377
34. Mariathasan, S., Ho, S. S., Zakarian, A., and Ohashi, P. S. (2000) *Eur J Immunol* **30**, 1060-1068
35. Li, Y. Q., Hii, C. S., Der, C. J., and Ferrante, A. (1999) *Immunology* **96**, 524-528
36. Hagemann, C., and Rapp, U. R. (1999) *Exp Cell Res* **253**, 34-46
37. Magnuson, N. S., Beck, T., Vahidi, H., Hahn, H., Smola, U., and Rapp, U. R.

(1994) *Semin Cancer Biol* **5**, 247-253

38. Eychene, A., Dusanter-Fourt, I., Barnier, J. V., Papin, C., Charon, M., Gisselbrecht, S., and Calothy, G. (1995) *Oncogene* **10**, 1159-1165
39. Barnier, J. V., Papin, C., Eychene, A., Lecoq, O., and Calothy, G. (1995) *J Biol Chem* **270**, 23381-23389
40. Wojnowski, L., Zimmer, A. M., Beck, T. W., Hahn, H., Bernal, R., Rapp, U. R., and Zimmer, A. (1997) *Nat Genet* **16**, 293-297
41. Papin, C., Eychene, A., Brunet, A., Pages, G., Pouyssegur, J., Calothy, G., and Barnier, J. V. (1995) *Oncogene* **10**, 1647-1651
42. Vaillancourt, R. R., Gardner, A. M., and Johnson, G. L. (1994) *Mol Cell Biol* **14**, 6522-6530
43. York, R. D., Yao, H., Dillon, T., Ellig, C. L., Eckert, S. P., McCleskey, E. W., and Stork, P. J. (1998) *Nature* **392**, 622-626
44. Brummer, T., Shaw, P. E., Reth, M., and Misawa, Y. (2002) *Embo J* **21**, 5611-5622
45. Erhardt, P., Schremser, E. J., and Cooper, G. M. (1999) *Mol Cell Biol* **19**, 5308-5315
46. Peraldi, P., Frodin, M., Barnier, J. V., Calleja, V., Scimeca, J. C., Filloux, C., Calothy, G., and Van Obberghen, E. (1995) *FEBS Lett* **357**, 290-296
47. Owaki, H., Varma, R., Gillis, B., Bruder, J. T., Rapp, U. R., Davis, L. S., and Geppert, T. D. (1993) *Embo J* **12**, 4367-4373
48. Northrop, J. P., Ullman, K. S., and Crabtree, G. R. (1993) *J Biol Chem* **268**, 2917-2923
49. van den Hoff, M. J., Moorman, A. F., and Lamers, W. H. (1992) *Nucleic Acids Res* **20**, 2902
50. Ohtsuka, T., Shimizu, K., Yamamori, B., Kuroda, S., and Takai, Y. (1996) *J Biol Chem* **271**, 1258-1261
51. Zhang, B. H., and Guan, K. L. (2000) *Embo J* **19**, 5429-5439
52. Boussiotis, V. A., Freeman, G. J., Berezovskaya, A., Barber, D. L., and Nadler, L. M. (1997) *Science* **278**, 124-128
53. Huang, Y., Boskovic, G., and Niles, R. M. (2003) *J Cell Physiol* **194**, 162-170

54. Ohtsuka, M., Arase, H., Takeuchi, A., Yamasaki, S., Shiina, R., Suenaga, T., Sakurai, D., Yokosuka, T., Arase, N., Iwashima, M., Kitamura, T., Moriya, H., and Saito, T. (2004) *Proc Natl Acad Sci U S A* **101**, 8126-8131
55. Tsygankov, A. Y. (2005) *J Cell Physiol* **203**,305-318
56. Tsukamoto, H., Irie, A., and Nishimura, Y. (2004) *J Biol Chem* **279**, 48457-48465
57. Katagiri, K., Shimonaka, M., and Kinashi, T. (2004) *J Biol Chem* **279**, 11875-11881
58. Uemura, Y., Senju, S., Maenaka, K., Iwai, L. K., Fujii, S., Tabata, H., Tsukamoto, H., Hirata, S., Chen, Y. Z., and Nishimura, Y. (2003) *J Immunol* **170**, 947-960
59. Rincon, M., Flavell, R. A., and Davis, R. J. (2001) *Oncogene* **20**, 2490-2497
60. Williams, B. L., Irvin, B. J., Sutor, S. L., Chini, C. C., Yacyshyn, E., Bubeck Wardenburg, J., Dalton, M., Chan, A. C., and Abraham, R. T. (1999) *Embo J* **18**, 1832-1844
61. Samelson, L. E. (2002) *Annu Rev Immunol* **20**, 371-394
62. Kitayama, H., Sugimoto, Y., Matsuzaki, T., Ikawa, Y., and Noda, M. (1989) *Cell* **56**, 77-84
63. Murphy, L. O., Smith, S., Chen, R. H., Fingar, D. C., and Blenis, J. (2002) *Nat Cell Biol* **4**, 556-564
64. Dumont, F. J., Staruch, M. J., Fischer, P., DaSilva, C., and Camacho, R. (1998) *J Immunol* **160**, 2579-2589
65. Pathan, N. I., Ashendel, C. L., Geahlen, R. L., and Harrison, M. L. (1996) *J Biol Chem* **271**, 30315-30317
66. Mason, C. S., Springer, C. J., Cooper, R. G., Superti-Furga, G., Marshall, C. J., and Marais, R. (1999) *Embo J* **18**, 2137-2148
67. Marais, R., Light, Y., Paterson, H. F., Mason, C. S., and Marshall, C. J. (1997) *J Biol Chem* **272**, 4378-4383
68. Vossler, M. R., Yao, H., York, R. D., Pan, M. G., Rim, C. S., and Stork, P. J. (1997) *Cell* **89**, 73-82
69. Miyoshi, H., Blomer, U., Takahashi, M., Gage, F. H., and Verma, I. M. (1998) *J Virol* **72**, 8150-8157

70. Costello, P. S., Walters, A. E., Mee, P. J., Turner, M., Reynolds, L. F., Prisco, A., Sarner, N., Zamoyska, R., and Tybulewicz, V. L. (1999) *Proc Natl Acad Sci U S A* **96**, 3035-3040
71. Xiang, X., Zang, M., Waelde, C. A., Wen, R., and Luo, Z. (2002) *J Biol Chem* **277**, 44996-45003
72. Chong, H., Lee, J., and Guan, K. L. (2001) *Embo J* **20**, 3716-3727
73. Borovsky, Z., Mishan-Eisenberg, G., Yaniv, E., and Rachmilewitz, J. (2002) *J Biol Chem* **277**, 21529-21536
74. Deng, T., and Karin, M. (1994) *Nature* **371**, 171-175
75. Genot, E., Cleverley, S., Henning, S., and Cantrell, D. (1996) *Embo J* **15**, 3923-3933
76. Reynolds, L. F., de Bettignies, C., Norton, T., Beeser, A., Chernoff, J., and Tybulewicz, V. L. (2004) *J Biol Chem* **279**, 18239-18246
77. Sebzda, E., Bracke, M., Tugal, T., Hogg, N., and Cantrell, D. A. (2002) *Nat Immunol* **3**, 251-258
78. Dillon, T. J., Karpitski, V., Wetzel, S. A., Parker, D. C., Shaw, A. S., and Stork, P. J. (2003) *J Biol Chem* **278**, 35940-35949
79. Villalba, M., Hernandez, J., Deckert, M., Tanaka, Y., and Altman, A. (2000) *Eur J Immunol* **30**, 1587-1596
80. Kuhne, M. R., Ku, G., and Weiss, A. (2000) *J Biol Chem* **275**, 2185-2190
81. Ernst, B., Lee, D. S., Chang, J. M., Sprent, J., and Surh, C. D. (1999) *Immunity* **11**, 173-181
82. Mariathasan, S., Zakarian, A., Bouchard, D., Michie, A. M., Zuniga-Pflucker, J. C., and Ohashi, P. S. (2001) *J Immunol* **167**, 4966-4973
83. Wojnowski, L., Stancato, L. F., Zimmer, A. M., Hahn, H., Beck, T. W., Larner, A. C., Rapp, U. R., and Zimmer, A. (1998) *Mech Dev* **76**, 141-149
84. Taylor-Fishwick, D. A., and Siegel, J. N. (1995) *Eur J Immunol* **25**, 3215-3221
85. Park, J. H., and Levitt, L. (1993) *Blood* **82**, 2470-2477
86. Porter, C. M., Havens, M. A., and Clipstone, N. A. (2000) *J Biol Chem* **275**, 3543-3551